iScience

CellPress
OPEN ACCESS

Article

Resolving neutrophils through genetic deletion of TRAM attenuate atherosclerosis pathogenesis

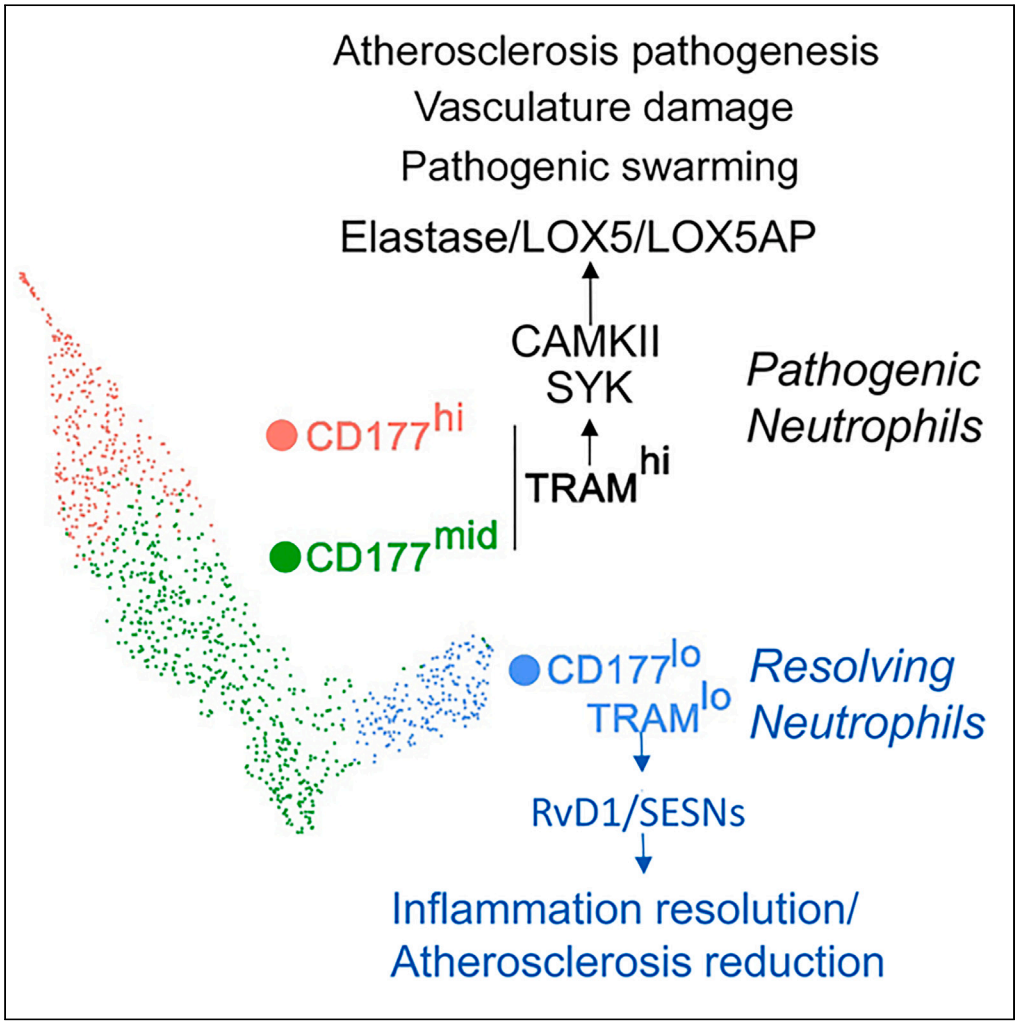

Shuo Geng, Yao Zhang, Ran Lu, Daniel Irimia, Liwu Li

lwli@vt.edu

Highlights

Both mice and human possess a resolving TRAM(Ticam2)^{lo} neutrophil subset

TRAM is a stress sensor for oxLDL and free cholesterol in neutrophil inflammation

TRAM$^{-/-}$ neutrophils express elevated anti-inflammatory resolving mediators

Transfusion of TRAM$^{-/-}$ neutrophils reduces experimental atherosclerosis

Geng et al., iScience 27, 110097
June 21, 2024
https://doi.org/10.1016/j.isci.2024.110097

iScience

CellPress
OPEN ACCESS

Article

Resolving neutrophils through genetic deletion of TRAM attenuate atherosclerosis pathogenesis

Shuo Geng,[1] Yao Zhang,[1] Ran Lu,[1] Daniel Irimia,[2] and Liwu Li[1,3,*]

SUMMARY

Systemic neutrophil dysregulation contributes to atherosclerosis pathogenesis, and restoring neutrophil homeostasis may be beneficial for treating atherosclerosis. Herein, we report that a homeostatic resolving subset of neutrophils exists in mice and humans characterized by the low expression of TRAM, correlated with reduced expression of inflammatory mediators (leukotriene B4 [LTB4] and elastase) and elevated expression of anti-inflammatory resolving mediators (resolvin D1 [RvD1] and CD200R). TRAM-deficient neutrophils can potently improve vascular integrity and suppress atherosclerosis pathogenesis when adoptively transfused into recipient atherosclerotic animals. Mechanistically, we show that TRAM deficiency correlates with reduced expression of 5-lipoxygenase (LOX5) activating protein (LOX5AP), dislodges nuclear localization of LOX5, and switches the lipid mediator secretion from pro-inflammatory LTB4 to pro-resolving RvD1. TRAM also serves as a stress sensor of oxidized low-density lipoprotein (oxLDL) and/or free cholesterol and triggers inflammatory signaling processes that facilitate elastase release. Together, our study defines a unique neutrophil population characterized by reduced TRAM, capable of homeostatic resolution and treatment of atherosclerosis.

INTRODUCTION

Despite extensive studies, atherosclerosis and related cardiovascular complications are a leading cause of morbidity and mortality worldwide.[1] Although a mechanistic link has been proposed between elevated circulating neutrophil counts and the development of atherosclerosis in both experimental animals and human patients,[2–4] this link is not sufficiently studied. Neutrophils account for ~50%–70% of human circulating leukocytes. In human atherosclerosis, high circulating neutrophil ratios have been tightly associated with characteristics of rupture-prone atherosclerotic lesions.[3,5,6] In experimental animals, neutrophilia promoted by hyperlipidemia accelerates early atherosclerosis.[7] Neutrophils contribute to atherosclerosis pathogenesis through enhanced adhesion to vasculatures and subsequent damage to endothelium via producing adhesion/swarming molecules such as leukotriene B4 (LTB4) and ICAM1, as well as tissue-degrading molecules such as myeloperoxidase (MPO) and elastase.[7–9] Depletion of inflammatory neutrophils reduces the atherosclerotic lesion burden.[7] Paradoxically, neutrophils are also beneficial during the resolution of inflammation through expressing resolving mediators such as resolvin D1 (RvD1).[10,11] Recent clinical studies reveal that the ratios of LTB4 vs. RvD1 closely correlate with clinical severity of cardiovascular diseases in human patients.[12,13] However, mechanisms underlying the paradoxical roles of neutrophils in promoting or resolving inflammation related to atherosclerosis pathogenesis and treatment are not well understood.

Key risk factors for atherosclerosis, such as oxidized low-density lipoprotein (oxLDL), as well as related oxidized phosphor-lipids (ox-PLs), are known to induce innate leukocyte activation through CD14/Toll-like receptor 4 (TLR4) in conjunction with other scavenger partners such as LOX1 and CD36.[14–20] In contrast to lipopolysaccharide (LPS), oxLDL/ox-PL-mediated CD14/TLR4 activation preferentially utilizes the unique downstream TRAM/TRIF instead of the MyD88 signaling pathways.[14–17,21] We and others independently validated that mice with TRAM or TRIF deletion instead of MyD88 drastically reduced atherosclerosis and other cardiovascular complications.[22–24] oxLDL triggers the activation of SYK/SRC kinases downstream of TRAM/TRIF, leading to the production of reactive oxygen species (ROS) and inflammatory mediators such as ICAM1 and CCR2 involved in the infiltration and adhesion of inflamed monocytes into atherosclerotic plaques.[23,25] Our integrated single-cell RNA sequencing (scRNA-seq) and biochemical studies reveal the important role of disrupted peroxisome homeostasis in low-grade inflammatory monocytes as the source of increased ROS and the signaling platform for SYK/SRC activation,[23] corroborated with recent findings of peroxisome serving as a key platform for sustaining inflammatory signaling.[26,27] In terms of neutrophils, however, signaling mechanisms responsible for its inflammatory activation triggered by oxLDL are less examined and understood.

[1]Department of Biological Sciences, Virginia Tech, Blacksburg VA 24061, USA
[2]Center for Engineering in Medicine & Surgery, Massachusetts General Hospital, Harvard Medical School, Shriners Burns Hospital, Boston, MA 02114, USA
[3]Lead contact
*Correspondence: lwli@vt.edu
https://doi.org/10.1016/j.isci.2024.110097

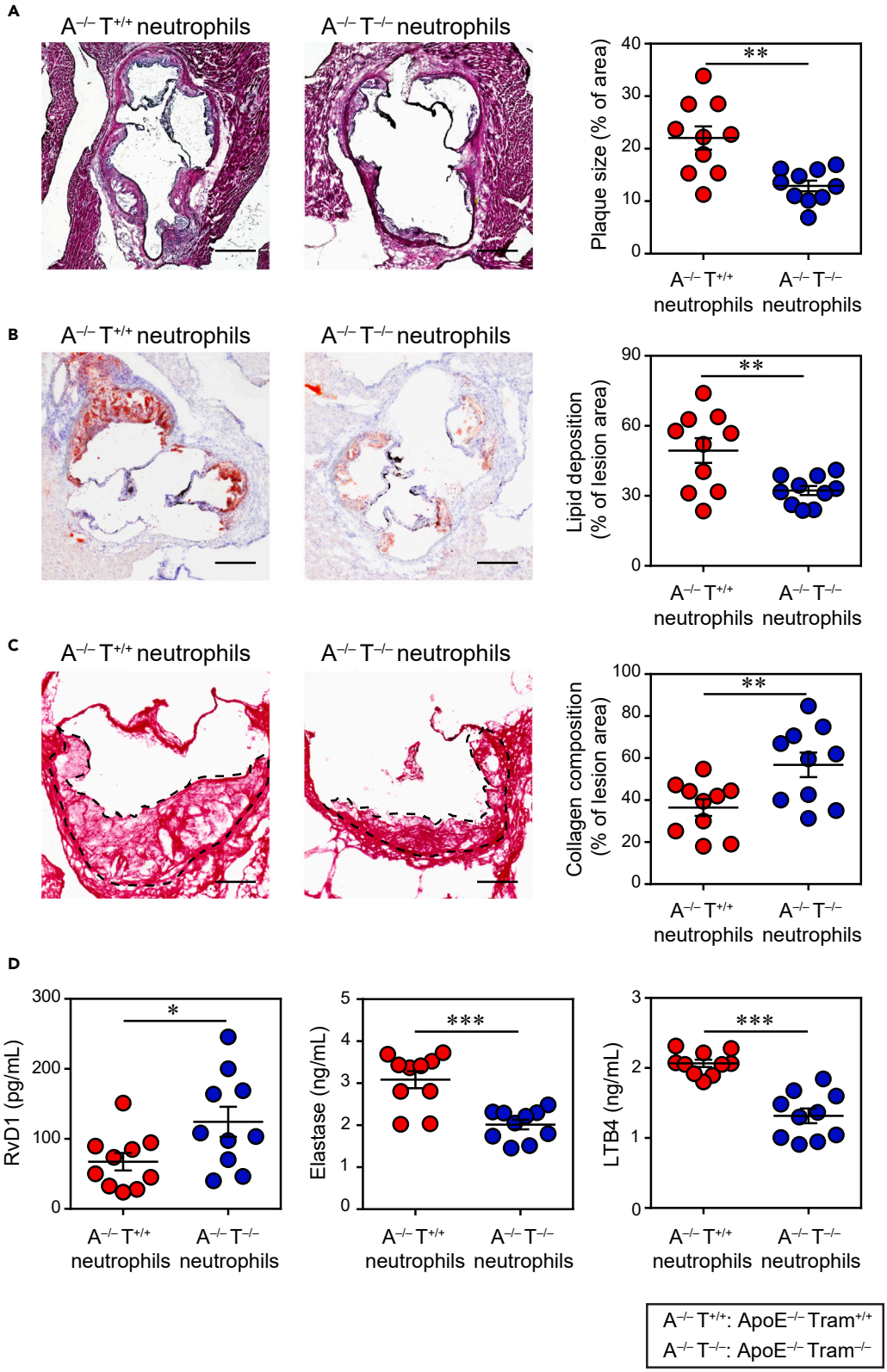
A
A−/− T+/+ neutrophils
A−/− T−/− neutrophils
Plaque size (% of area)
**
A−/− T+/+ neutrophils
A−/− T−/− neutrophils
B
A−/− T+/+ neutrophils
A−/− T−/− neutrophils
Lipid deposition (% of lesion area)
**
A−/− T+/+ neutrophils
A−/− T−/− neutrophils
C
A−/− T+/+ neutrophils
A−/− T−/− neutrophils
Collagen composition (% of lesion area)
**
A−/− T+/+ neutrophils
A−/− T−/− neutrophils
D
RvD1 (pg/mL)
*
A−/− T+/+ neutrophils
A−/− T−/− neutrophils
Elastase (ng/mL)
***
A−/− T+/+ neutrophils
A−/− T−/− neutrophils
LTB4 (ng/mL)
***
A−/− T+/+ neutrophils
A−/− T−/− neutrophils
A−/− T+/+: ApoE−/− Tram+/+
A−/− T−/−: ApoE−/− Tram−/−

Figure 1. Transfusion of Tram$^{-/-}$ neutrophils ameliorates atherosclerosis

Male ApoE$^{-/-}$ Tram$^{+/+}$ recipient mice were first fed with HFD for 4 weeks. Neutrophils isolated from ApoE$^{-/-}$ Tram$^{+/+}$ mice or Apoe$^{-/-}$ Tram$^{-/-}$ mice were adoptively transferred by intravenous injection to HFD-fed recipient mice once a week for an additional 4 weeks. Samples were collected 1 week after the last neutrophil transfer.

(A) Representative images of H&E-stained atherosclerotic lesions and quantification of plaque size demonstrated as the percentage of lesion area within aortic root area. Scale bar, 300 μm.

(B) Representative images of oil red O-stained atherosclerotic plaques and quantification of lipid deposition within the lesion area. Scale bar, 300 μm.

(C) Representative images of Picrosirius red-stained atherosclerotic plaques and quantification of collagen content within lesion area. Scale bar, 100 μm.

(D) Determination of plasma RevD1, elastase, and LTB4 levels by ELISA. Data are presented as means ± SEM. *$p < 0.05$, **$p < 0.01$, and ***$p < 0.001$; Student's 2-tailed t test ($n = 10$ for each group).

We recently identified TRAM as a critical mediator controlling neutrophil inflammatory activation.[28] Independent scRNA-seq studies revealed three subsets of mature circulating neutrophils in mice and humans,[28,29] with two majority subsets exhibiting inflammatory/pro-apoptotic/degranulation characteristics and one minor subset of anti-inflammatory resolving neutrophils.[28] Our comparative analyses revealed that the resolving neutrophils express not only less inflammatory mediators and caspases but also resolving mediators such as RvD1, CD200R, and Sestrin1 (SESN1).[28] RvD1 serves as an effective lipid-resolving mediator capable of reducing tissue inflammation.[30] CD200R can suppress inter-cellular inflammatory activation.[23] SESN1 is a potent suppressor of oxLDL-mediated inflammasome activation[31] and subsequent degranulation.[32] Intriguingly, we observed that TRAM is only highly expressed in the majority subsets of inflammatory/apoptotic neutrophils and is absent in the minor population of resolving neutrophils. Consequently, we studied the effect of the genetic deletion of TRAM and found that it reprograms neutrophils into the resolving state.[28]

Here, we show that TRAM is a crucial switch toggling the generation of pro-inflammatory and resolving neutrophils. Given its therapeutic potential, we systematically characterized the resolving characteristics of Tram$^{-/-}$ neutrophils and the potential of Tram$^{-/-}$ neutrophils for treating experimental atherosclerosis.

RESULTS

Transfusion of Tram$^{-/-}$ neutrophils alleviates the pathogenesis of atherosclerosis in mice

Given our previous findings that TRAM deletion can effectively reprogram neutrophils into the resolving state with enhanced expression of anti-inflammatory mediators such as RvD1 and CD200R,[28,33,34] we hypothesized that Tram$^{-/-}$ neutrophils may be harnessed therapeutically to treat experimental atherosclerosis. We tested this hypothesis by performing neutrophil transfusion studies with the atherosclerosis-prone recipient mice. We used male and female ApoE$^{-/-}$ Tram$^{+/+}$ mice as recipient mice and fed them with a high-fat diet (HFD) for 4 weeks. Then, the mice received intravenous injections of neutrophils purified from the bone marrow of either ApoE$^{-/-}$ Tram$^{-/-}$ mice or control ApoE$^{-/-}$ Tram$^{+/+}$ mice. The adoptive transfer of neutrophils was performed weekly for 4 weeks, and the recipient mice received HFD for the entire experiment. The mice were sacrificed for analysis 1 week after the final neutrophil injection. Histological assessments through hematoxylin and eosin staining and oil red O staining revealed that both male and female mice receiving the transfer of Tram$^{-/-}$ neutrophils had a significant reduction in plaque sizes (Figures 1A and S1A) as well as remarkably decreased lipid deposition area within atherosclerotic lesions (Figures 1B and S1B) as compared to the counterparts receiving Tram$^{+/+}$ neutrophils. Moreover, Picrosirius red staining demonstrated a significantly elevated level of collagen content in plaques following the adoptive transfer of ApoE$^{-/-}$ Tram$^{-/-}$ neutrophils in comparison to ApoE$^{-/-}$ Tram$^{+/+}$ neutrophils (Figures 1C and S1C). The recipient mice transfused with Tram$^{+/+}$ neutrophils demonstrated comparable histological characteristics ($p > 0.05$), including plaque size and lipid deposition, as compared to the sham ApoE$^{-/-}$ mice that were fed with HFD as we published previously.[23]

We measured the plasma levels of key mediators produced by neutrophils. Notably, adoptive transfer of ApoE$^{-/-}$ Tram$^{-/-}$ neutrophils led to a significant elevation in the secretion of resolving product RvD1. This was accompanied by a significant decrease in the secretion of pro-inflammatory mediators such as LTB4, elastase, and MPO (Figures 1D and S2A). To test the recruitment of injected neutrophils to the aorta, we labeled ApoE$^{-/-}$ Tram$^{+/+}$ and ApoE$^{-/-}$ Tram$^{-/-}$ neutrophils with CFSE before transfusion. Subsequently, we detected a small but distinct CFSE^{+} Ly6G^{+} neutrophil population in the mice that received the transfusion, and the injection of neutrophils did not significantly alter the frequency of total aortic neutrophils (Figure S3).

The plasma levels of total cholesterol, free cholesterol, and triglyceride were comparable between the mice injected with ApoE$^{-/-}$ Tram$^{+/+}$ neutrophils and those injected with ApoE$^{-/-}$ Tram$^{-/-}$ neutrophils (Figure S4). However, the administration of ApoE$^{-/-}$ Tram$^{-/-}$ neutrophils remarkably reduced the plasma levels of tumor necrosis factor alpha and CCL5 (Figure S2B), both of which play critical roles in atherosclerosis development.[35,36] Interestingly, injection of ApoE$^{-/-}$ Tram$^{-/-}$ neutrophils significantly decreased the expression of pro-inflammatory markers such as ICAM1 and CD38 on the surface of bone marrow and splenic monocytes (Figure S5). These findings suggested that administrating ApoE$^{-/-}$ Tram$^{-/-}$ neutrophils attenuated systemic inflammation in atherosclerotic mice, potentially contributing to the alleviation of atherosclerosis pathogenesis.

Our data indicate that adoptive transfer of Tram$^{-/-}$ neutrophils can effectively mitigate atherosclerosis progression and strengthen the stability of atherosclerotic plaques. This approach may serve as a potential avenue for immune cell therapy in the treatment of atherosclerosis. These observed effects may be associated with the alteration of neutrophil functionalities from a pro-inflammatory state to a resolution state caused by TRAM deficiency. Since there was no gender disparity in the effectiveness of neutrophil transfusion, we only used male ApoE$^{-/-}$ Tram$^{+/+}$ mice as recipients in the following *in vivo* studies.

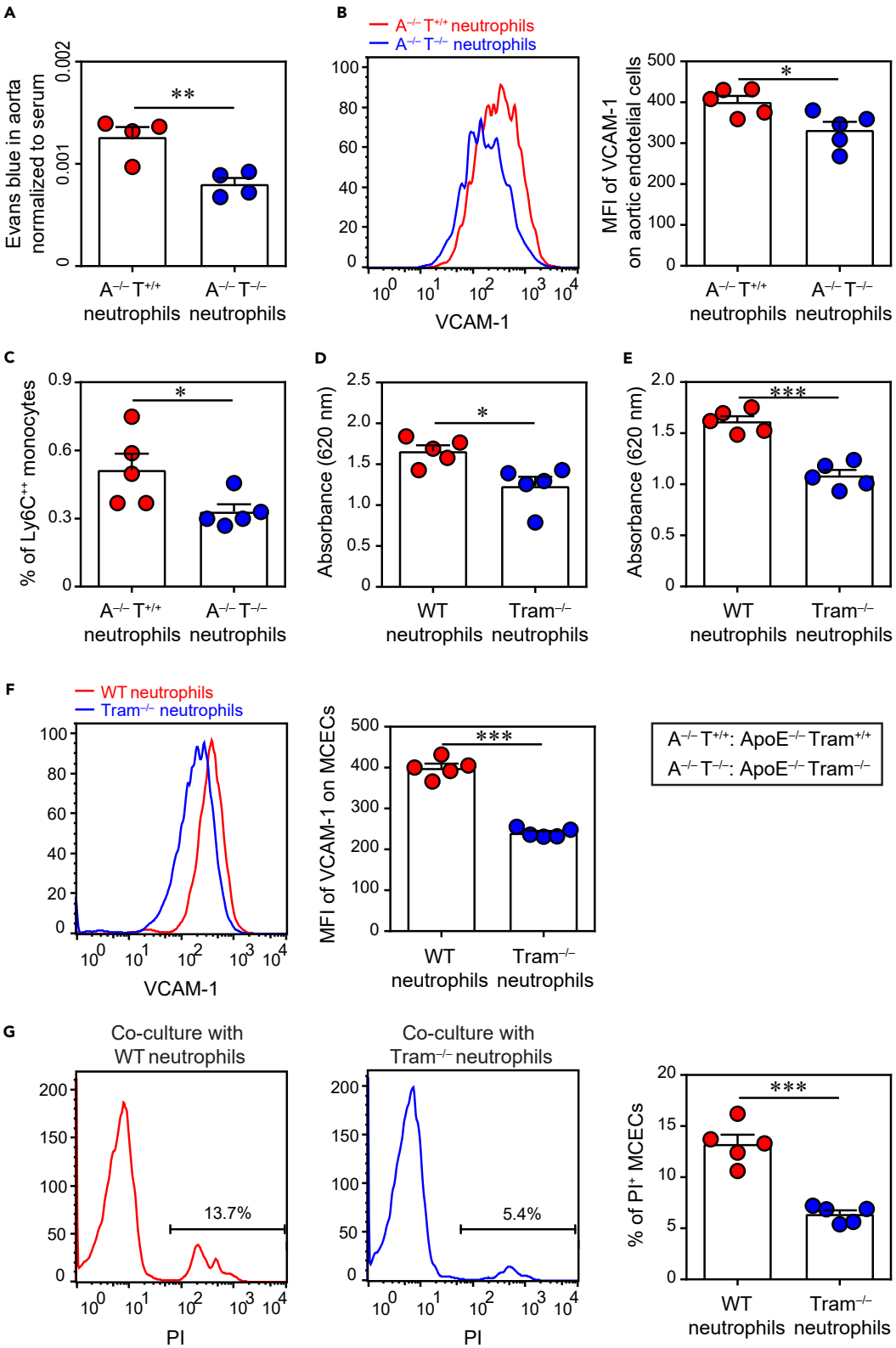
A
Evans blue in aorta normalized to serum
0.002
0.001
0
**
A−/− T+/+ neutrophils
A−/− T−/− neutrophils
B
A−/− T+/+ neutrophils
A−/− T−/− neutrophils
100
80
60
40
20
0
10^0 10^1 10^2 10^3 10^4
VCAM-1
MFI of VCAM-1 on aortic endotelial cells
500
400
300
200
100
0
*
A−/− T+/+ neutrophils
A−/− T−/− neutrophils
C
% of Ly6C++ monocytes
0.9
0.6
0.3
0
*
A−/− T+/+ neutrophils
A−/− T−/− neutrophils
D
Absorbance (620 nm)
2.5
2.0
1.5
1.0
0.5
0
*
WT neutrophils
Tram−/− neutrophils
E
Absorbance (620 nm)
2.0
1.5
1.0
0.5
0
***
WT neutrophils
Tram−/− neutrophils
F
WT neutrophils
Tram−/− neutrophils
100
80
60
40
20
0
10^0 10^1 10^2 10^3 10^4
VCAM-1
MFI of VCAM-1 on MCECs
500
400
300
200
100
0
***
WT neutrophils
Tram−/− neutrophils
A−/− T+/+: ApoE−/− Tram+/+
A−/− T−/−: ApoE−/− Tram−/−
G
Co-culture with WT neutrophils
200
150
100
50
0
13.7%
10^0 10^1 10^2 10^3 10^4
PI
Co-culture with Tram−/− neutrophils
200
150
100
50
0
5.4%
10^0 10^1 10^2 10^3 10^4
PI
% of PI+ MCECs
20
15
10
5
0
***
WT neutrophils
Tram−/− neutrophils

Figure 2. Tram$^{-/-}$ neutrophils exert protective effects on endothelial cells

(A–C) ApoE$^{-/-}$ Tram$^{+/+}$ recipient mice were first fed with HFD for 4 weeks. Neutrophils isolated from ApoE$^{-/-}$ Tram$^{+/+}$ mice or ApoE$^{-/-}$ Tram$^{-/-}$ mice were adoptively transferred by intravenous injection to HFD-fed recipient mice once a week for an additional 4 weeks. (A) One week after the final cell transfer, Evans blue solution was intravenously injected, and Evans blue leaked into the aorta was analyzed (n = 4). (B) VCAM-1 expression on aortic endothelial cells was analyzed by fluorescence-activated cell sorting (FACS). Representative FACS histogram and quantification are displayed (n = 5). (C) FACS analysis of Ly6C^{++} pro-inflammatory monocyte frequency in the aorta (n = 5).

(D) WT or Tram$^{-/-}$ murine neutrophils were co-cultured with the monolayer of bend.3 cells in a Transwell system for 24 h. Evans blue leakage to the lower chambers was determined by the absorbance at 620 nm (n = 5).

(E) WT or Tram$^{-/-}$ murine neutrophils were co-cultured with the monolayer of MCECs in a Transwell system for 24 h. Evans blue leakage to the lower chambers was determined by the absorbance at 620 nm (n = 5).

(F) WT or Tram$^{-/-}$ murine neutrophils were co-cultured with MCECs for 24 h, and VCAM-1 expression on MCECs was analyzed by FACS. Representative FACS histogram and quantification are displayed (n = 5).

(G) WT or Tram$^{-/-}$ murine neutrophils were co-cultured with MCECs for 24 h, and the death of MCECs was determined by propidium iodide (PI) staining. Representative FACS histogram and quantification are displayed (n = 5). Data are presented as means ± SEM. *p < 0.05, **p < 0.01, and ***p < 0.001; Student's 2-tailed t test.

Transfusion of Tram$^{-/-}$ neutrophils effectively improves vasculature integrity

It has been extensively documented that the disrupted function and integrity of the arterial endothelial cell crucially contributes to the development of atherosclerosis.[37,38] Neutrophil elastase has been identified as a factor that increases the permeability of endothelial cells,[39] while RvD1 exerts a robust protective effect in enhancing endothelial integrity and barrier function.[40] With our findings that Tram$^{-/-}$ neutrophils exhibit elevated levels of RvD1 and reduced secretion of elastase,[28] and our *in vivo* adoptive transfer data revealing elevated plasma levels of RvD1 and reduced elastase in recipient mice receiving Tram$^{-/-}$ neutrophils, we then tested whether Tram$^{-/-}$ neutrophils may improve vascular integrity. We found that 1 week after the final cell transfer, the atherosclerotic mice receiving the transfusion of ApoE$^{-/-}$ Tram$^{-/-}$ neutrophils had significantly reduced transvascular leak, measured by Evans blue accumulation in the aorta, compared with the mice receiving ApoE$^{-/-}$ Tram$^{+/+}$ neutrophils (Figure 2A).

We also assessed the expression of VCAM-1, a pro-inflammatory molecule crucial for atherosclerosis development,[41] on the surface of aortic endothelial cells. Flow cytometry analysis revealed that adoptive transfer of ApoE$^{-/-}$ Tram$^{-/-}$ neutrophils dramatically decreased VCAM-1 expression on the endothelial cells (Figures 2B and S6A), accompanied by a notable reduction of Ly6C^{++} pro-inflammatory monocyte infiltration into the aorta (Figure 2C). These data suggest that transfusion of TRAM-deficient neutrophils effectively enhances vascular endothelial integrity and alleviates the pro-inflammatory state of endothelial cells in atherosclerotic mice.

We next sought to verify the protective effects of Tram$^{-/-}$ neutrophils on endothelial cells *in vitro*. To exclude the possible influence of differential apoptotic rates between wild-type (WT) or Tram$^{-/-}$ neutrophils, we assessed the viability of neutrophils within our culture system. Consistent with our previous report, over 95% of cultured neutrophils remained viable after *in vitro* culture for 24 (Figure S7A) and 48 h (Figure S7B). Moreover, no significant difference in viability was observed between WT and Tram$^{-/-}$ neutrophils. We then measured the leakage of Evans blue in an *in vitro* Transwell-Evans blue permeability assay.[42,43] For this, we cultured bEnd.3 cells, an endothelial cell line derived from the mouse brain, and MCE cells (immortalized mouse cardiac endothelial cells [MCECs]) on inserts to form a monolayer. Then, we co-cultured these with neutrophils purified from WT or Tram$^{-/-}$ mice. We measured the leakage of Evans blue from the upper chamber to the lower chamber and found a significant reduction in Evans blue amounts in the lower chambers when endothelial cells were co-cultured with Tram$^{-/-}$ neutrophils compared to those co-cultured with WT neutrophils (Figures 2D and 2E), indicating that TRAM deficiency in neutrophils substantially enhances the integrity of both bEnd.3 and MCEC layers.

In line with the *in vivo* observations, co-culture of Tram$^{-/-}$ neutrophils led to a significantly decreased expression of VCAM-1 on the surface of diverse endothelial cell types, including MCECs (Figures 2F and S6B), bEnd.3 cells (Figure S8A), as well as human umbilical vein endothelial cells (Figure S8B). The death of endothelial cells is a pivotal initiating event in atherogenesis. While the atherosclerotic plaques contain abundant apoptotic endothelial cells,[44] we speculated that Tram$^{-/-}$ neutrophils may exert a protective effect by attenuating the death of cardiac endothelial cells. Indeed, our flow cytometry analysis unveiled a significantly higher viability of MCECs when co-cultured with Tram$^{-/-}$ neutrophils compared to those co-cultured with WT neutrophils (Figure 2G). Together, these results unveiled the critical role of TRAM expressed by neutrophils in modulating endothelial cells toward an atherosclerosis-prone state, and its deficiency emerges as a potential therapeutic target for preventing and treating atherosclerosis.

TRAM deletion reduces FLAP expression and dislodges LOX5 away from the nuclear membrane into the cytosol

Considering the elevated RvD1 level in the circulation of atherosclerotic mice post-transfusion of Tram$^{-/-}$ neutrophils, we reasoned that Tram$^{-/-}$ neutrophils may be the primary source of RvD1. Incubation with oxLDL remarkably attenuated RvD1 production by WT neutrophils, while, conversely, Tram$^{-/-}$ neutrophils exhibited resistance to oxLDL-mediated suppression of RvD1 production. Moreover, the baseline RvD1 production of Tram$^{-/-}$ neutrophils surpassed that of their WT counterparts, suggesting that TRAM functions as a negative modulator of RvD1 production in neutrophils and that the absence of TRAM leads to constitutive production of high levels of RvD1 (Figure 3A).

We examined key molecular mechanisms involved in the elevated generation of RvD1 in Tram$^{-/-}$ neutrophils. By surveying the scRNA-seq data in our previous published study,[28] we noticed a drastically reduced expression of 5-lipoxygenase (LOX5) activating protein (Lox5ap) (FLAP) in the naturally occurring TRAM^{lo} neutrophil subset (Figure S9). FLAP is a key molecule responsible for anchoring LOX5 onto the

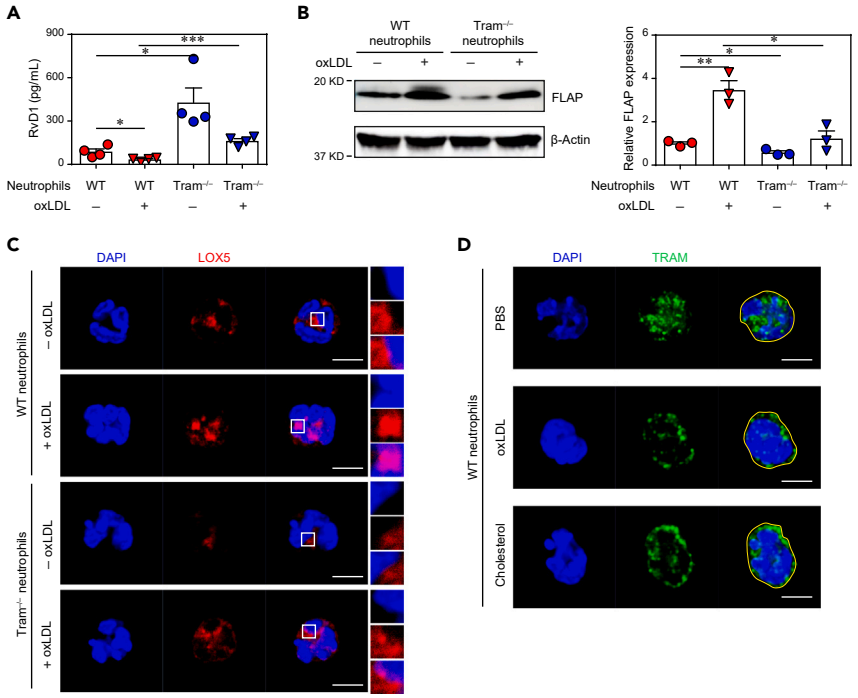

Figure 3. TRAM deletion reduces FLAP expression and impedes the nuclear distribution of LOX5 in neutrophils

WT and Tram$^{-/-}$ murine neutrophils were treated with oxLDL (10 μg/mL) or cholesterol (10 μg/mL) for 48 h.

(A) Secretion of RevD1 by neutrophils was quantified by ELISA (n = 4).

(B) Protein level of FLAP was examined by western blotting, and relative expression was normalized to β-actin (n = 3).

(C) Confocal microscopy imaging of the subcellular distribution of LOX5 in neutrophils. Scale bar, 5 μm.

(D) Confocal microscopy imaging of the subcellular distribution of TRAM in neutrophils. Scale bar, 5 μm. Data are presented as means ± SEM. *p < 0.05, **p < 0.01, and ***p < 0.001; one-way ANOVA.

nuclear membrane and enabling the production of inflammatory mediator LTB4.[45] On the other hand, when LOX5 is not anchored on the nuclear membrane, cytosolic LOX5 is channeled into generating the resolving lipid mediator RvD1.[46] Through immunoblot analyses, we validated that Tram$^{-/-}$ neutrophils expressed significantly less FLAP protein than WT neutrophils under steady-state conditions. Upon priming with oxLDL, a substantial elevation in FLAP protein expression was observed in WT neutrophils, while, in contrast, oxLDL-induced FLAP increase was significantly attenuated in Tram$^{-/-}$ neutrophils (Figure 3B).

We further performed confocal microscopy to examine the subcellular distribution of LOX5. As expected, we observed that WT neutrophils preferentially expressed LOX5 within the nuclear membrane area, and oxLDL treatment elevated the nuclear-membrane-associated LOX5 protein. In sharp contrast, we observed that TRAM deletion disrupted the nuclear localization of LOX5 (Figures 3C and S10A).

TRAM is widely recognized as an adaptor protein for TLRs. However, the role of TRAM expressed by neutrophils in mediating atherosclerotic stress and the inflammatory effects of lipids is less well understood. Current literature suggests that oxLDL or cholesterol can cause generic membrane stress,[47,48] and TRAM is one of the few innate membrane adaptors with lipid anchors to stressed membrane region.[49] Thus, we reasoned that TRAM may also serve as a general membrane stress sensor for oxLDL and free cholesterol, in addition to TLR ligands. Our confocal microscopy examination yielded compelling evidence supporting such a role for TRAM. We found that both oxLDL and free cholesterol treatment induced a remarkable translocation of TRAM in neutrophils and promoted TRAM clustering on the cell membrane (Figure 3D).

These data unveiled the potential role of TRAM as a sensor for diverse lipid-induced membrane stress, which induces the translocation of LOX5 from cytosol to nucleus and subsequently suppresses RvD1 production. TRAM deletion can reverse these events, restoring RvD1 production and facilitating inflammation resolution.

RvD1 mediates the endothelial protective effects of Tram$^{-/-}$ neutrophils

We further hypothesized that the elevated RvD1 secretion by Tram$^{-/-}$ neutrophils may be crucial for their endothelial protective effects. To test this, we first blocked direct contact between neutrophils and endothelial cells in the co-culture system using a transwell insert, which separated neutrophils in the upper chamber from MCECs in the lower chamber. Remarkably, Tram$^{-/-}$ neutrophils, even when physically separated from MCECs, dramatically reduced endothelial VCAM-1 expression (Figure 4A) and inhibited the death of MCECs (Figure 4B), demonstrating

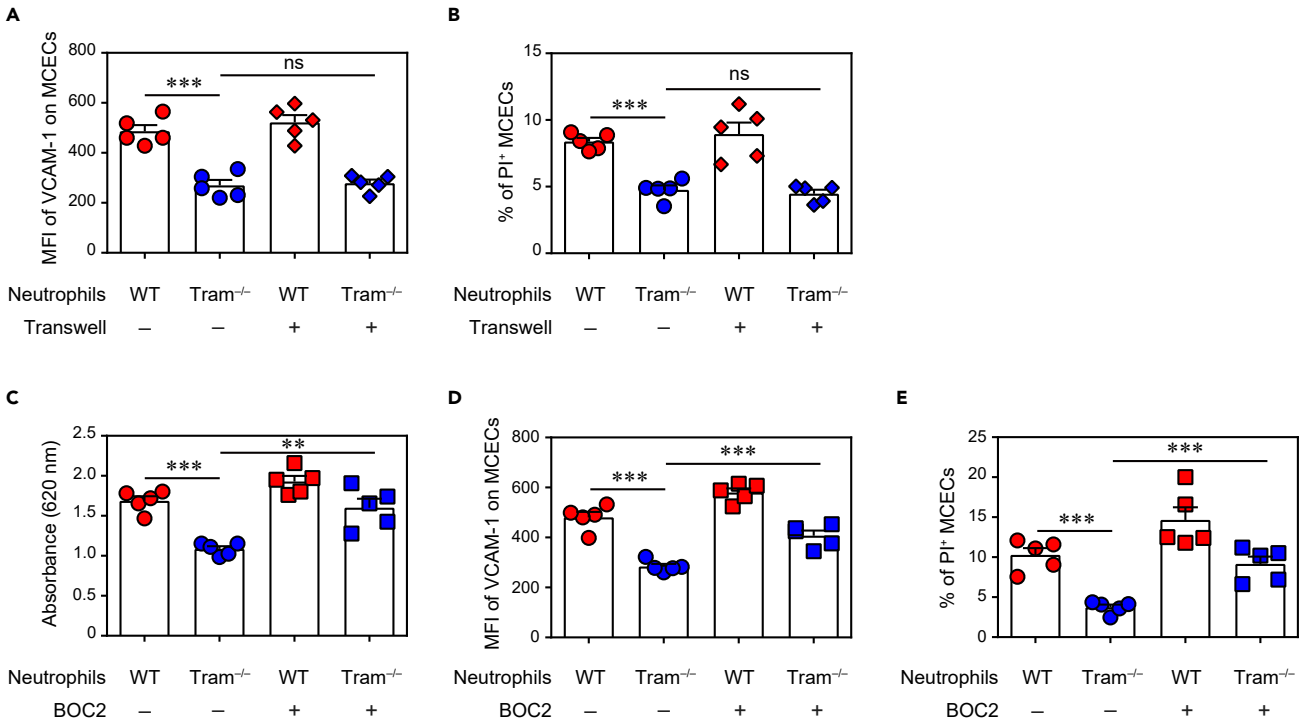

Figure 4. Secreted RvD1 is indispensable to the endothelial protective effects of Tram$^{-/-}$ neutrophils

(A and B) WT or Tram$^{-/-}$ murine neutrophils were directly co-cultured with MCECs. Alternatively, the neutrophils were seeded in the upper chamber and MCECs were seeded in the lower chamber of a Transwell system. (A) After culture for 24 h, VCAM-1 expression on MCECs was analyzed by FACS (n = 5). (B) The death of MCECs was determined by PI staining (n = 5).

(C) The monolayer of MCECs in a Transwell system was pre-incubated with BOC2 (10 μM) or vehicle buffer for 1 h, and then co-cultured with WT or Tram$^{-/-}$ murine neutrophils for 24 h. Evans blue leakage to the lower chambers was determined by the absorbance at 620 nm (n = 5).

(D) MCECs were pre-incubated with BOC2 (10 μM) or vehicle buffer for 1 h, and then co-cultured with WT or Tram$^{-/-}$ murine neutrophils for 24 h. VCAM-1 expression on MCECs was analyzed by FACS (n = 5).

(E) MCECs were pre-incubated with BOC2 (10 μM) or vehicle buffer for 1 h, and then co-cultured with WT or Tram$^{-/-}$ murine neutrophils for 24 h. The death of MCECs was determined by PI staining (n = 5). Data are presented as means ± SEM. ns non-significant, *p < 0.05, **p < 0.01, and ***p < 0.001; one-way ANOVA.

effects comparable to Tram$^{-/-}$ neutrophils freely contacted with endothelial cells. These results suggest that direct neutrophil-endothelial cell contact may not be essential for the protective effects of Tram$^{-/-}$ neutrophils.

Next, we further tested whether secreted RvD1 from resolving neutrophils may be involved in the observed effect. The monolayer of MCECs was pre-incubated with BOC2, a specific inhibitor for RvD1 receptor ALX/FPR2,[50] followed by co-culture with neutrophils and analysis of Evans blue leakage. We found that BOC2 significantly abrogated protective effect of Tram$^{-/-}$ neutrophils on endothelial integrity (Figure 4C). In addition, blockade of RvD1 receptor also significantly attenuated the efficacy of Tram$^{-/-}$ neutrophils in reducing VCAM-1 expression on MCECs (Figure 4D) and preventing MCEC death (Figure 4E). Taken together, these data suggest that the endothelial protective effects of Tram$^{-/-}$ neutrophils were dependent on the secretion of RvD1.

TRAM deletion increases the expression of SESN1 and reduces the expression of SYK, CaMKII, and elastase in mouse neutrophils

Neutrophil elastase plays a crucial role in the pathogenesis of atherosclerosis, with all neutrophils in atherosclerotic lesions exhibiting a high expression of elastase.[51,52] Our *in vivo* data revealed that the adoptive transfer of Tram$^{-/-}$ neutrophils led to decreased elastase in atherosclerotic mice. Specifically, we observed that the elastase release from Tram$^{-/-}$ neutrophils was significantly diminished compared to that from WT neutrophils, both with and without oxLDL treatment (Figure 5A). We further examined the molecular mechanisms responsible for the reduced secretion of elastase from Tram$^{-/-}$ neutrophils. First, we tested the potential role of cellular ROS as mediators of neutrophil elastase secretion, as suggested by previous reports.[53] We found that oxLDL induced ROS generation in WT neutrophils, and TRAM deletion attenuated the ROS induction (Figure 5B). Second, we tested if TRAM may function as a sensor for lipid-induced stress, based on previous studies suggesting that peroxisome disruption is a key trigger for inflammatory signaling and intracellular ROS accumulation.[54] Additionally, we demonstrated that TRAM had the capability to transmit the signal of super-low dose LPS, leading to peroxisomal dysfunction.[23] Here, we performed confocal imaging analyses of pexophagy in neutrophils treated with oxLDL. In WT neutrophils, oxLDL treatment drastically

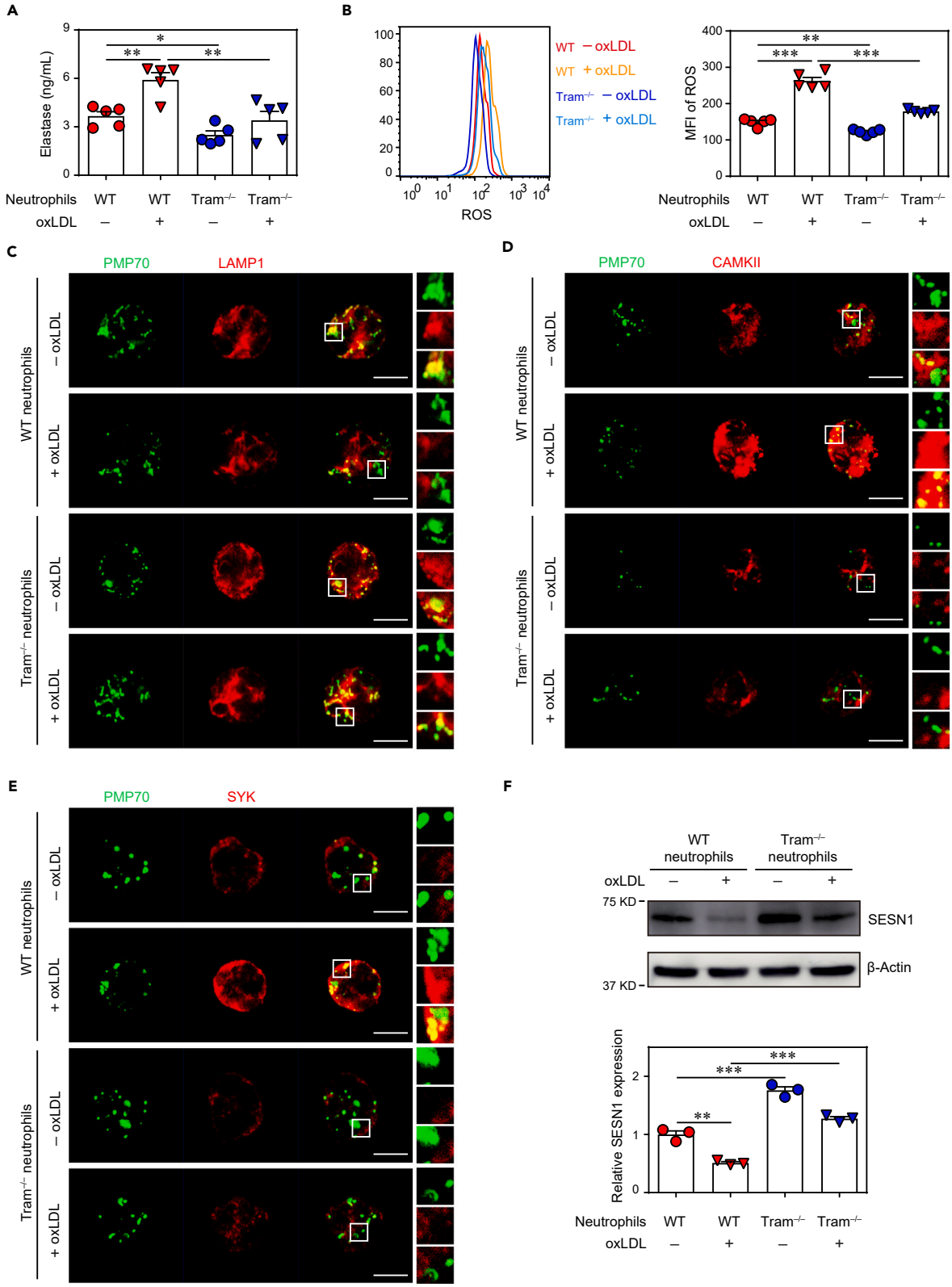
A
Elastase (ng/mL)
Neutrophils WT WT Tram−/− Tram−/−
oxLDL – + – +
B
WT – oxLDL
WT + oxLDL
Tram−/− – oxLDL
Tram−/− + oxLDL
ROS
MFI of ROS
C
PMP70
LAMP1
WT neutrophils
Tram−/− neutrophils
– oxLDL
+ oxLDL
D
PMP70
CAMKII
E
PMP70
SYK
F
WT neutrophils
Tram−/− neutrophils
oxLDL
75 KD
SESN1
37 KD
β-Actin
Relative SESN1 expression

Figure 5. TRAM deletion abrogates the molecular machineries responsible for elastase production

WT and Tram$^{-/-}$ murine neutrophils were treated with oxLDL (10 μg/mL) for 48 h.

(A) Secretion of elastase by neutrophils was quantified by ELISA (n = 5).

(B) Neutrophils were labeled with CellROX, and ROS levels were quantified by FACS (n = 5).

(C) Neutrophils were stained with anti-PMP70 and anti-LAMP1 antibodies, and the localization of peroxisomes and lysosomes was examined by confocal microcopy. Scale bar, 5 μm.

(D) Confocal microscopy imaging of the subcellular distribution of PMP70^{+} peroxisomes and CaMKII in neutrophils. Scale bar, 5 μm.

(E) Confocal microscopy imaging of the subcellular distribution of PMP70^{+} peroxisomes and SYK in neutrophils. Scale bar, 5 μm.

(F) Protein level of SESN1 was examined by western blotting, and relative expression was normalized to β-actin (n = 3). Data are presented as means ± SEM. *p < 0.05, **p < 0.01, and ***p < 0.001; one-way ANOVA.

disrupted the fusion of peroxisomes (PMP70^{+}) and lysosomes (LAMP1^{+}); Tram$^{-/-}$ neutrophils exhibited constitutively elevated peroxisome-lysosome fusion, and this fusion was minimally affected by oxLDL (Figures 5C and S10B). Activation of calmodulin-dependent kinase II (CaMKII) by metabolic stress is known to catalyze the transformation of glucose into ROS.[55,56] Our western blot results revealed that oxLDL treatment significantly increased the expression of CaMKII (Figure S11A) and the SRC kinase SYK (Figure S11B) in WT neutrophils. Confocal analysis demonstrated that oxLDL potently increased the localization of CaMKII at peroxisomes in WT neutrophils (Figures 5D and S10C). Moreover, oxLDL also increased the peroxisomal distribution of SYK (Figures 5E and S10D), which was shown to form a mutually activating positive feedback loop with subcellular ROS. These findings align with previous studies, demonstrating the crucial role of peroxisomes as a platform for sustaining the inflammatory signaling cascade.[57,58] Importantly, oxLDL failed to not only elevate the protein expression of CaMKII and SYK (Figure S11) but also induce CaMKII and SYK aggregation around peroxisomes in TRAM-deficient neutrophils (Figures 5D, 5E, S10C, and S10D). Collectively, our data reveal that TRAM is responsible for oxLDL-mediated disruption of pexophagy, and induction of inflammatory signaling processes responsible for the neutrophil release of elastase.

In addition to ROS, inflammasome activation also triggers the release of neutrophil granules.[59] We noticed from our scRNA-seq data that TRAM-deficient neutrophils have elevated expression of SESN1 (Figure S9), a key homeostatic molecule capable of suppressing inflammasome activation.[31] Previous studies reveal a mutually suppressive circuit among inflammatory signals (STAT1/5) vs. anti-inflammatory signals (PPAR/PGC1α/β).[23,60–62] We demonstrated that TRAM deletion not only reduced the inflammatory STAT1/5 signals, but also elevated anti-inflammatory PPAR/PGC1 signals,[28] which are known to induce the expression of anti-inflammatory SESN1.[63] We then performed an immunoblot assay and validated the increased expression of SESN1 in TRAM-deficient compared to WT neutrophils. Moreover, oxLDL treatment remarkably increased SESN1 expression in WT neutrophils but had minimal impact on Tram$^{-/-}$ neutrophils in terms of SESN1 level (Figure 5F). Together, our data suggest that reduced peroxisome-associated inflammatory signaling coupled with elevated homeostatic mediator SESN1 may collectively lead to reduced elastase secretion in TRAM-deficient neutrophils.

Human neutrophil subset with reduced TRAM expression exhibits a similar phenotype of improved homeostasis *ex vivo*

To examine the human relevance of our findings, we tested the correlations between TRAM, activation marker CD177, elastase, and LTB4 secretion, in human neutrophils *ex vivo*. Fresh neutrophils from healthy human donors segregated into CD177^{hi} and CD177^{lo} populations, consistent with scRNA-seq data conserved from mice to humans.[28,29] We then co-stained with a TRAM-specific antibody and observed that TRAM is preferentially expressed in CD177 ^{hi} neutrophils and largely absent from the CD177^{lo} neutrophils (Figure 6A), consistent with our findings with murine neutrophils.

We further evaluated the functional relevance of human neutrophils with reduced TRAM expression. Since inflammatory neutrophils with higher expression of LTB4 and CD11b tend to exhibit exacerbated swarming ability,[64] we tested the swarming potential of sorted human neutrophils. As shown in Figure 6, human CD177^{hi} neutrophils accumulated faster and in higher numbers on the swarming targets than CD177^{lo} neutrophils (Figure 6B, Videos S1 and S2). We further subject human neutrophils to *ex vivo* priming with fMLP to elicit the secretion of pro-inflammatory mediators, such as LTB4 and elastase. Both human CD177^{lo} and CD177^{hi} neutrophils were capable of secreting LTB4 and elastase in response to fMLP treatment. However human CD177^{lo} neutrophils secreted significantly less LTB4 and elastase as compared to CD177^{hi} neutrophils, consistent with the observation of reduced swarming ability of CD177^{lo} neutrophils (Figures 6C and 6D).

DISCUSSION

Our study identified resolving neutrophils capable of improving vasculature integrity and reducing atherosclerosis. Our results suggest that TRAM serves as a stress sensor of oxLDL and/or free cholesterol and that deficiencies in the expression of TRAM reduce the expression of inflammatory mediators (LTB4 and elastase) and elevate the expression of anti-inflammatory resolving mediators (RvD1 and CD200R). Mechanistically, we show that TRAM deficiency correlates with reduced expression of LOX5AP, dislodged nuclear localization of LOX5, the release of pro-resolving RvD1, and reduced ability to swarm.

Our findings harken to the era of immune cell-based precision therapies for chronic inflammatory diseases. Although conventional therapies against atherosclerosis based on small chemicals or biological molecules have been widely developed, there are intrinsic caveats associated with these approaches, as reflected in systemic side effects and limited delivery efficacies. Innate immune leukocytes such as neutrophils are naturally equipped with tissue tropic capabilities to effectively survey and home into inflamed areas.[65,66] Emerging studies attempted utilizing neutrophil-based approaches in delivering therapeutic compounds to treat diseases.[67] However, neutrophils exhibit diverse inflammatory characteristics, including degranulation and release of inflammatory mediators, swarming, and aggregation with

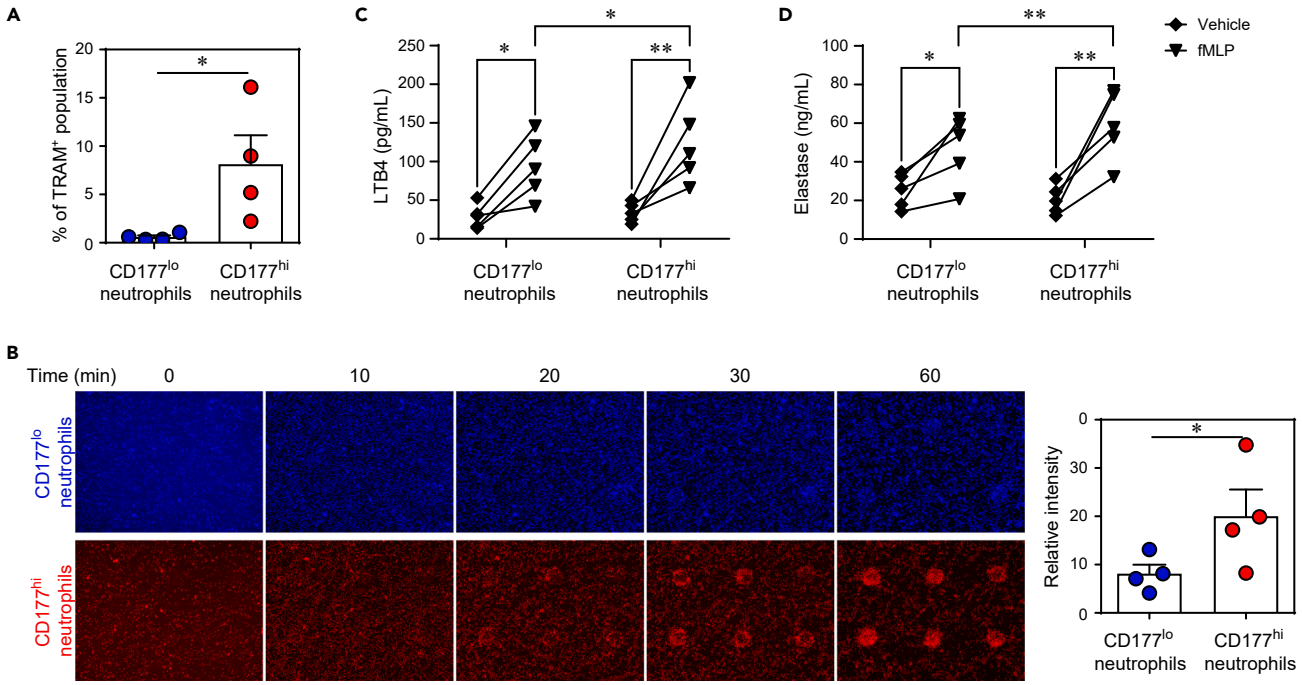

Figure 6. Human CD177^{lo} neutrophils exhibit similar resolving characteristics to mouse Tram$^{-/-}$ neutrophils

(A) FACS analysis of TRAM^{+} population frequency in CD66b^{+} CD177^{lo} and CD66b^{+} CD177^{hi} neutrophils from the peripheral blood of healthy individuals (n = 4).

(B) CD177^{lo} and CD177^{hi} neutrophils were purified from the peripheral blood of healthy individuals. CD177^{lo} neutrophils were labeled with Hoechst 33342, and CD177^{hi} neutrophils were labeled with DRAQ5. The swarming of the neutrophils was recorded and quantified (n = 4).

(C and D) Purified CD177^{lo} and CD177^{hi} neutrophils were stimulated with or without fMLP (100 nM) for 4 h. The secretion of LTB4 (C) and elastase (D) was analyzed by ELISA (n = 5). Data are presented as means ± SEM. *p < 0.05 and **p < 0.01; Student's 2-tailed t test.

neighboring cells and tissues.[66,68,69] These tissue-toxic effects of neutrophils hinder the proper development of neutrophil-based delivery or cell therapies. Our integrated scRNA-seq and functional analyses identified a unique subset of neutrophils with potent homeostatic resolving capability enabled by TRAM reduction.

Our findings complement emerging independent reports demonstrating the therapeutic potential of homeostatic neutrophils in treating chronic diseases.[70–73] A recent study reports that a subset of CD177^{lo} "young" neutrophils is effective in treating stroke when directly injected into the hippocampus region of experimental animals and that the levels of CD177^{lo} "young" neutrophils are drastically reduced in patients.[74] On the other hand, CD177^{hi} neutrophils are independently shown to be apoptotic[75] and elevated in patients with severe infections such as COVID-related complications.[76] Validating these reports, our scRNA-seq data revealed that CD177^{Pos} neutrophils express elevated levels of apoptotic genes such as Casp1 and 3, in addition to inflammatory mediators such as Lox5AP (FLAP). In contrast, the CD177^{lo} neutrophils express higher levels of anti-apoptotic genes such as MCL1, as well as inflammasome/degranulation suppressors such as SESN1/3. We observed that TRAM is absent in the CD177^{lo} "young" neutrophils and that genetic deletion of TRAM can enable the expansion of resolving neutrophils with therapeutic potential for improving vasculature integrity and treating atherosclerosis. Our data further suggest that resolving neutrophils may likely contribute to tissue homeostasis and atherosclerosis resolution through both systemic and local effects. Transfusion of resolving neutrophils leads to a systemic improvement of vasculature integrity *in vivo*. Through blocking RvD1 receptor, our complementary *in vitro* mechanistic data support the systemic paracrine role of resolving neutrophils on improving endothelial integrity through secreted mediator. Although it is well known that there are very few neutrophils within plaques, we did observe the infiltration of transfused resolving neutrophils inside the plaques. Analyses of resident immune cells reveal that transfusion of resolving neutrophils leads to the re-programming of local immune cells with homeostatic characteristics, suggesting potential local communication among resolving neutrophils with resident immune cells. Therefore, it is likely that transfused neutrophils can be applied to exhibit both systemic and local effects, with further studies needed to characterize their relative contributions.

Mechanistically, our data reveal that TRAM contributes to inflammatory/apoptotic neutrophil polarization through mediating peroxisome-mediated activation of SYK and CaMKII, leading to the induction of LOX5AP. This is consistent with previous mechanistic studies that demonstrate the spatial regulation of inflammatory LTB4 vs. anti-inflammatory RvD1 expression.[77] Nuclear localization of LOX5 controlled by LOX5AP enables the production of LTB4, while cytosolic LOX5 participates in the generation of RvD1.[46,78] TRAM-mediated inflammatory signaling can also trigger inflammasome activation and degranulation, which leads to the enhanced release of tissue-damaging elastase. Elevated plasma levels of elastase were shown to induce endothelial damage, which is the early cause of atherosclerosis initiation.[79] Our data further clarify an important principle by which neutrophils sense cholesterol stress. Although TRAM was initially identified as a signaling

adaptor for the TLR4-mediated innate signaling process,[80] later studies suggest that TRAM can serve as a generic stress sensor for diverse stress signals, including ox-PL.[49] TRAM is a unique signaling adaptor with a covalently conjugated lipid moiety, which enables TRAM to sense membrane stress mediated by lipid-raft formation.[81,82] Both oxLDL and free cholesterol increased membrane stress and affected lipid-raft formation.[83] This may explain why TRAM can serve as a general stress sensor, including oxLDL. Consistent with these observations, we observed that oxLDL can potently induce the membrane clustering of TRAM on neutrophils. Our data provide an important clue that targeting TRAM membrane clustering may hold future potential for designing effective intervention strategies in treating chronic low-grade inflammation and atherosclerosis. TRAM membrane clustering is mediated by covalent myristoylation, and inhibitors that can suppress such process may be developed to treat atherosclerosis in future studies.

Our studies with primary human neutrophils reveal that the CD177^{lo} neutrophils subset correlates with reduced TRAM expression, confirming our observations with murine neutrophils. Our functional assays validate that the human CD177^{lo} TRAM neutrophils exhibit reduced inflammatory characteristics, including reduced swarming and reduced secretion of inflammatory elastase, as compared to CD177^{hi} neutrophils. Our data suggest that elutriation of human CD177^{lo} neutrophils may have therapeutic potential in treating human chronic cardiovascular diseases. Future functional studies are needed to better define promising neutrophil subsets amenable to neutrophil-based cell therapies.

Limitations of the study

Our current work serves as an initial examination of neutrophils with resolving characteristics, defines a key role of TRAM in serving as a fundamental switch in modulating the generation of resolving neutrophils in both murine and human systems, and provides an initial proof of principle of applying resolving neutrophils in an animal model of atherosclerosis. We were able to maintain robust *ex vivo* neutrophil survival with the supplement of G-CSF and demonstrated the beneficial effects of transfused neutrophils in reducing experimental atherosclerosis. However, we caution that future systems studies are needed to better define their therapeutic potential. Additional characterization of pharmacodynamics and pharmacokinetics parameters with temporal and spatial resolution is needed to define the systemic and local effects of various neutrophil subsets. Transfused neutrophils likely interact with recipient cells and tissues in a complex fashion and either directly or indirectly affect host immune metabolism. The immune-metabolic axis was beyond the scope of this current study and will require future comprehensive analyses. Furthermore, although human and murine neutrophils share some key mechanistic features as we noted, human neutrophils may be more prone to apoptosis and less amenable to therapeutic application. Neutrophils engineered from stem cells should be considered to generate sufficient human neutrophils with either genetic alteration of TRAM or targeted chemical inhibition of TRAM membrane conjugation, for the next phase of translational considerations.

STAR★METHODS

Detailed methods are provided in the online version of this paper and include the following:

- KEY RESOURCES TABLE
- RESOURCE AVAILABILITY
  - Lead contact
  - Materials availability
  - Data and code availability
- EXPERIMENTAL MODEL AND STUDY PARTICIPANT DETAILS
  - Animals and ethics statement
- METHOD DETAILS
  - Primary murine neutrophil culture
  - Human neutrophils isolation
  - Cell lines
  - HFD feeding and neutrophil adoptive transfer
  - Histological analyses of atherosclerotic lesions
  - ELISA
  - Determination of plasma lipids
  - Flow cytometry analysis of aortic neutrophils
  - Assessment of aortic endothelium permeability
  - Flow cytometry analysis of aortic endothelial cells
  - Flow cytometry analysis of bone marrow and splenic monocytes
  - Assessment of the viability of neutrophils cultured *in vitro*
  - Neutrophil-endothelial cell co-culture, Transwell-Evans Blue permeability assay, and flow cytometry analysis
  - Assessment of the infleuce of neutrophils on endothrelial cells without direct cell-cell contact
  - Immunoblotting
  - Confocal microscopy
  - Detection of intracellular ROS

- Flow cytometry analyses of human neutrophils
- Swarming assay
- QUANTIFICATION AND STATISTICAL ANALYSIS

SUPPLEMENTAL INFORMATION

Supplemental information can be found online at https://doi.org/10.1016/j.isci.2024.110097.

ACKNOWLEDGMENTS

The authors would like to acknowledge the assistance of Feng Xu, Ziyue Yi, Jacqueline Hou, and other Li lab members for animal breeding and care, as well as technical assistance. This study was supported in part by National Institutes of Health grants HL163948 to L.L. and GM092804 to D.I.

AUTHOR CONTRIBUTIONS

S.G. and L.L. designed the study. S.G., Y.Z., and R.L. performed the experiments. S.G., Y.Z., D.I., and L.L. provided reagents and/or analyzed the data. S.G. and L.L. wrote the manuscript.

DECLARATION OF INTERESTS

The authors declare no competing interests.

Received: December 26, 2023
Revised: April 23, 2024
Accepted: May 21, 2024
Published: May 24, 2024

REFERENCES

1. Virani, S.S., Alonso, A., Aparicio, H.J., Benjamin, E.J., Bittencourt, M.S., Callaway, C.W., Carson, A.P., Chamberlain, A.M., Cheng, S., Delling, F.N., et al. (2021). Heart Disease and Stroke Statistics-2021 Update: A Report From the American Heart Association. Circulation *143*, e254–e743. https://doi.org/10.1161/CIR.0000000000000950.
2. Silvestre-Roig, C., Braster, Q., Ortega-Gomez, A., and Soehnlein, O. (2020). Neutrophils as regulators of cardiovascular inflammation. Nat. Rev. Cardiol. *17*, 327–340. https://doi.org/10.1038/s41569-019-0326-7.
3. Adamstein, N.H., MacFadyen, J.G., Rose, L.M., Glynn, R.J., Dey, A.K., Libby, P., Tabas, I.A., Mehta, N.N., and Ridker, P.M. (2021). The neutrophil-lymphocyte ratio and incident atherosclerotic events: analyses from five contemporary randomized trials. Eur. Heart J. *42*, 896–903. https://doi.org/10.1093/eurheartj/ehaa1034.
4. Mawhin, M.A., Tilly, P., Zirka, G., Charles, A.L., Slimani, F., Vonesch, J.L., Michel, J.B., Bäck, M., Norel, X., and Fabre, J.E. (2018). Neutrophils recruited by leukotriene B4 induce features of plaque destabilization during endotoxaemia. Cardiovasc. Res. *114*, 1656–1666. https://doi.org/10.1093/cvr/cvy130.
5. Nam, K.W., Kwon, H.M., Jeong, H.Y., Park, J.H., Kim, S.H., and Jeong, S.M. (2018). High neutrophil to lymphocyte ratios predict intracranial atherosclerosis in a healthy population. Atherosclerosis *269*, 117–121. https://doi.org/10.1016/j.atherosclerosis.2017.12.035.
6. Ionita, M.G., van den Borne, P., Catanzariti, L.M., Moll, F.L., de Vries, J.P.P.M., Pasterkamp, G., Vink, A., and de Kleijn, D.P.V. (2010). High neutrophil numbers in human carotid atherosclerotic plaques are associated with characteristics of rupture-prone lesions. Arterioscler. Thromb. Vasc. Biol. *30*, 1842–1848. https://doi.org/10.1161/ATVBAHA.110.209296.
7. Drechsler, M., Megens, R.T.A., van Zandvoort, M., Weber, C., and Soehnlein, O. (2010). Hyperlipidemia-triggered neutrophilia promotes early atherosclerosis. Circulation *122*, 1837–1845. https://doi.org/10.1161/CIRCULATIONAHA.110.961714.
8. Rotzius, P., Thams, S., Soehnlein, O., Kenne, E., Tseng, C.N., Björkström, N.K., Malmberg, K.J., Lindbom, L., and Eriksson, E.E. (2010). Distinct infiltration of neutrophils in lesion shoulders in ApoE-/- mice. Am. J. Pathol. *177*, 493–500. https://doi.org/10.2353/ajpath.2010.090480.
9. Li, J., Kumari, T., Barazia, A., Jha, V., Jeong, S.Y., Olson, A., Kim, M., Lee, B.K., Manickam, V., Song, Z., et al. (2022). Neutrophil DREAM promotes neutrophil recruitment in vascular inflammation. J. Exp. Med. *219*, e20211083. https://doi.org/10.1084/jem.20211083.
10. Casanova-Acebes, M., Nicolás-Ávila, J.A., Li, J.L., García-Silva, S., Balachander, A., Rubio-Ponce, A., Weiss, L.A., Adrover, J.M., Burrows, K., A-González, N., et al. (2018). Neutrophils instruct homeostatic and pathological states in naive tissues. J. Exp. Med. *215*, 2778–2795. https://doi.org/10.1084/jem.20181468.
11. Filep, J.G., and Ariel, A. (2020). Neutrophil heterogeneity and fate in inflamed tissues: implications for the resolution of inflammation. Am. J. Physiol. Cell Physiol. *319*, C510–C532. https://doi.org/10.1152/ajpcell.00181.2020.
12. Thul, S., Labat, C., Temmar, M., Benetos, A., and Bäck, M. (2017). Low salivary resolvin D1 to leukotriene B4 ratio predicts carotid intima media thickness: A novel biomarker of non-resolving vascular inflammation. Eur. J. Prev. Cardiol. *24*, 903–906. https://doi.org/10.1177/2047487317694464.
13. Welty, F.K., Schulte, F., Alfaddagh, A., Elajami, T.K., Bistrian, B.R., and Hardt, M. (2021). Regression of human coronary artery plaque is associated with a high ratio of (18-hydroxy-eicosapentaenoic acid + resolvin E1) to leukotriene B4. Faseb. J. *35*, e21448. https://doi.org/10.1096/fj.202002471R.
14. Imai, Y., Kuba, K., Neely, G.G., Yaghubian-Malhami, R., Perkmann, T., van Loo, G., Ermolaeva, M., Veldhuizen, R., Leung, Y.H.C., Wang, H., et al. (2008). Identification of oxidative stress and Toll-like receptor 4 signaling as a key pathway of acute lung injury. Cell *133*, 235–249. https://doi.org/10.1016/j.cell.2008.02.043.
15. Wiesner, P., Choi, S.H., Almazan, F., Benner, C., Huang, W., Diehl, C.J., Gonen, A., Butler, S., Witztum, J.L., Glass, C.K., and Miller, Y.I. (2010). Low doses of lipopolysaccharide and minimally oxidized low-density lipoprotein cooperatively activate macrophages via nuclear factor kappa B and activator protein-1: possible mechanism for acceleration of atherosclerosis by subclinical endotoxemia. Circ. Res. *107*, 56–65. CIRCRESAHA.110.218420. https://doi.org/10.1161/CIRCRESAHA.110.218420.
16. Bae, Y.S., Lee, J.H., Choi, S.H., Kim, S., Almazan, F., Witztum, J.L., and Miller, Y.I. (2009). Macrophages generate reactive oxygen species in response to minimally oxidized low-density lipoprotein: toll-like receptor 4- and spleen tyrosine kinase-dependent activation of NADPH oxidase 2. Circ. Res. *104*, 210–218. 221p following 218. https://doi.org/10.1161/CIRCRESAHA.108.181040.

17. Di Gioia, M., Spreafico, R., Springstead, J.R., Mendelson, M.M., Joehanes, R., Levy, D., and Zanoni, I. (2020). Endogenous oxidized phospholipids reprogram cellular metabolism and boost hyperinflammation. Nat. Immunol. *21*, 42–53. https://doi.org/10.1038/s41590-019-0539-2.
18. Nowicki, M., Müller, K., Serke, H., Kosacka, J., Vilser, C., Ricken, A., and Spanel-Borowski, K. (2010). Oxidized low-density lipoprotein (oxLDL)-induced cell death in dorsal root ganglion cell cultures depends not on the lectin-like oxLDL receptor-1 but on the toll-like receptor-4. J. Neurosci. Res. *88*, 403–412. https://doi.org/10.1002/jnr.22205.
19. Stewart, C.R., Stuart, L.M., Wilkinson, K., van Gils, J.M., Deng, J., Halle, A., Rayner, K.J., Boyer, L., Zhong, R., Frazier, W.A., et al. (2010). CD36 ligands promote sterile inflammation through assembly of a Toll-like receptor 4 and 6 heterodimer. Nat. Immunol. *11*, 155–161. ni.1836. https://doi.org/10.1038/ni.1836.
20. Cao, D., Luo, J., Chen, D., Xu, H., Shi, H., Jing, X., and Zang, W. (2016). CD36 regulates lipopolysaccharide-induced signaling pathways and mediates the internalization of Escherichia coli in cooperation with TLR4 in goat mammary gland epithelial cells. Sci. Rep. *6*, 23132. https://doi.org/10.1038/srep23132.
21. Zanoni, I., and Granucci, F. (2013). Role of CD14 in host protection against infections and in metabolism regulation. Front. Cell. Infect. Microbiol. *3*, 32. https://doi.org/10.3389/fcimb.2013.00032.
22. Lundberg, A.M., Ketelhuth, D.F.J., Johansson, M.E., Gerdes, N., Liu, S., Yamamoto, M., Akira, S., and Hansson, G.K. (2013). Toll-like receptor 3 and 4 signalling through the TRIF and TRAM adaptors in haematopoietic cells promotes atherosclerosis. Cardiovasc. Res. *99*, 364–373. https://doi.org/10.1093/cvr/cvt033.
23. Geng, S., Zhang, Y., Yi, Z., Lu, R., and Li, L. (2021). Resolving monocytes generated through TRAM deletion attenuate atherosclerosis. JCI Insight *6*, e149651. https://doi.org/10.1172/jci.insight.149651.
24. Vorkapic, E., Lundberg, A.M., Mäyränpää, M.I., Eriksson, P., and Wågsäter, D. (2015). TRIF adaptor signaling is important in abdominal aortic aneurysm formation. Atherosclerosis *241*, 561–568. https://doi.org/10.1016/j.atherosclerosis.2015.06.014.
25. Klionsky, D.J., Abdel-Aziz, A.K., Abdelfatah, S., Abdellatif, M., Abdoli, A., Abel, S., Abeliovich, H., Abildgaard, M.H., Abudu, Y.P., Acevedo-Arozena, A., et al. (2021). Guidelines for the use and interpretation of assays for monitoring autophagy (4th edition)[1]. Autophagy *17*, 1–382. https://doi.org/10.1080/15548627.2020.1797280.
26. Odendall, C., Dixit, E., Stavru, F., Bierne, H., Franz, K.M., Durbin, A.F., Boulant, S., Gehrke, L., Cossart, P., and Kagan, J.C. (2014). Diverse intracellular pathogens activate type III interferon expression from peroxisomes. Nat. Immunol. *15*, 717–726. https://doi.org/10.1038/ni.2915.
27. Vasko, R., Ratliff, B.B., Bohr, S., Nadel, E., Chen, J., Xavier, S., Chander, P., and Goligorsky, M.S. (2013). Endothelial peroxisomal dysfunction and impaired pexophagy promotes oxidative damage in lipopolysaccharide-induced acute kidney injury. Antioxid. Redox Signal. *19*, 211–230. https://doi.org/10.1089/ars.2012.4768.
28. Lin, R., Yi, Z., Wang, J., Geng, S., and Li, L. (2022). Generation of resolving memory neutrophils through pharmacological training with 4-PBA or genetic deletion of TRAM. Cell Death Dis. *13*, 345. https://doi.org/10.1038/s41419-022-04809-6.
29. Xie, X., Shi, Q., Wu, P., Zhang, X., Kambara, H., Su, J., Yu, H., Park, S.Y., Guo, R., Ren, Q., et al. (2020). Single-cell transcriptome profiling reveals neutrophil heterogeneity in homeostasis and infection. Nat. Immunol. *21*, 1119–1133. https://doi.org/10.1038/s41590-020-0736-z.
30. Spite, M., Clària, J., and Serhan, C.N. (2014). Resolvins, specialized proresolving lipid mediators, and their potential roles in metabolic diseases. Cell Metab. *19*, 21–36. https://doi.org/10.1016/j.cmet.2013.10.006.
31. Keping, Y., Yunfeng, S., Pengzhuo, X., Liang, L., Chenhong, X., and Jinghua, M. (2020). Sestrin1 inhibits oxidized low-density lipoprotein-induced activation of NLRP3 inflammasome in macrophages in a murine atherosclerosis model. Eur. J. Immunol. *50*, 1154–1166. https://doi.org/10.1002/eji.201948427.
32. Shin, J., Pan, H., and Zhong, X.P. (2012). Regulation of mast cell survival and function by tuberous sclerosis complex 1. Blood *119*, 3306–3314. https://doi.org/10.1182/blood-2011-05-353342.
33. Huang, A., Young, T.L., Dang, V.T., Shi, Y., McAlpine, C.S., and Werstuck, G.H. (2017). 4-phenylbutyrate and valproate treatment attenuates the progression of atherosclerosis and stabilizes existing plaques. Atherosclerosis *266*, 103–112. https://doi.org/10.1016/j.atherosclerosis.2017.09.034.
34. Lin, R., Wang, J., Wu, Y., Yi, Z., Zhang, Y., and Li, L. (2023). Resolving neutrophils due to TRAM deletion renders protection against experimental sepsis. Inflamm. Res. *72*, 1733–1744. https://doi.org/10.1007/s00011-023-01779-z.
35. Kim, C.W., Oh, E.T., and Park, H.J. (2021). A strategy to prevent atherosclerosis via TNF receptor regulation. Faseb. J. *35*, e21391. https://doi.org/10.1096/fj.202000764R.
36. Amadori, L., Calcagno, C., Fernandez, D.M., Koplev, S., Fernandez, N., Kaur, R., Mury, P., Khan, N.S., Sajja, S., Shamailova, R., et al. (2023). Systems immunology-based drug repurposing framework to target inflammation in atherosclerosis. Nat. Cardiovasc. Res. *2*, 550–571. https://doi.org/10.1038/s44161-023-00278-y.
37. Gimbrone, M.A., Jr., and García-Cardeña, G. (2016). Endothelial Cell Dysfunction and the Pathobiology of Atherosclerosis. Circ. Res. *118*, 620–636. https://doi.org/10.1161/CIRCRESAHA.115.306301.
38. Chistiakov, D.A., Orekhov, A.N., and Bobryshev, Y.V. (2015). Endothelial Barrier and Its Abnormalities in Cardiovascular Disease. Front. Physiol. *6*, 365. https://doi.org/10.3389/fphys.2015.00365.
39. Liu, H., Lessieur, E.M., Saadane, A., Lindstrom, S.I., Taylor, P.R., and Kern, T.S. (2019). Neutrophil elastase contributes to the pathological vascular permeability characteristic of diabetic retinopathy. Diabetologia *62*, 2365–2374. https://doi.org/10.1007/s00125-019-04998-4.
40. Chattopadhyay, R., Raghavan, S., and Rao, G.N. (2017). Resolvin D1 via prevention of ROS-mediated SHP2 inactivation protects endothelial adherens junction integrity and barrier function. Redox Biol. *12*, 438–455. https://doi.org/10.1016/j.redox.2017.02.023.
41. Nakashima, Y., Raines, E.W., Plump, A.S., Breslow, J.L., and Ross, R. (1998). Upregulation of VCAM-1 and ICAM-1 at atherosclerosis-prone sites on the endothelium in the ApoE-deficient mouse. Arterioscler. Thromb. Vasc. Biol. *18*, 842–851. https://doi.org/10.1161/01.atv.18.5.842.
42. Friedl, J., Puhlmann, M., Bartlett, D.L., Libutti, S.K., Turner, E.N., Gnant, M.F.X., and Alexander, H.R. (2002). Induction of permeability across endothelial cell monolayers by tumor necrosis factor (TNF) occurs via a tissue factor-dependent mechanism: relationship between the procoagulant and permeability effects of TNF. Blood *100*, 1334–1339.
43. Zheng, X., Zhang, W., and Hu, X. (2018). Different concentrations of lipopolysaccharide regulate barrier function through the PI3K/Akt signalling pathway in human pulmonary microvascular endothelial cells. Sci. Rep. *8*, 9963. https://doi.org/10.1038/s41598-018-28089-3.
44. Choy, J.C., Granville, D.J., Hunt, D.W., and McManus, B.M. (2001). Endothelial cell apoptosis: biochemical characteristics and potential implications for atherosclerosis. J. Mol. Cell. Cardiol. *33*, 1673–1690. https://doi.org/10.1006/jmcc.2001.1419.
45. Subramanian, B.C., Majumdar, R., and Parent, C.A. (2017). The role of the LTB(4)-BLT1 axis in chemotactic gradient sensing and directed leukocyte migration. Semin. Immunol. *33*, 16–29. https://doi.org/10.1016/j.smim.2017.07.002.
46. Lehmann, C., Homann, J., Ball, A.K., Blöcher, R., Kleinschmidt, T.K., Basavarajappa, D., Angioni, C., Ferreirós, N., Häfner, A.K., Rådmark, O., et al. (2015). Lipoxin and resolvin biosynthesis is dependent on 5-lipoxygenase activating protein. Faseb. J. *29*, 5029–5043. https://doi.org/10.1096/fj.15-275487.
47. Couto, N.F., Rezende, L., Fernandes-Braga, W., Alves, A.P., Agero, U., Alvarez-Leite, J., Damasceno, N.R.T., Castro-Gomes, T., and Andrade, L.O. (2020). OxLDL alterations in endothelial cell membrane dynamics leads to changes in vesicle trafficking and increases cell susceptibility to injury. Biochim. Biophys. Acta Biomembr. *1862*, 183139. https://doi.org/10.1016/j.bbamem.2019.183139.
48. Chakraborty, S., Doktorova, M., Molugu, T.R., Heberle, F.A., Scott, H.L., Dzikovski, B., Nagao, M., Stingaciu, L.R., Standaert, R.F., Barrera, F.N., et al. (2020). How cholesterol stiffens unsaturated lipid membranes. Proc. Natl. Acad. Sci. USA *117*, 21896–21905. https://doi.org/10.1073/pnas.2004807117.
49. Barnett, K.C., and Kagan, J.C. (2020). Lipids that directly regulate innate immune signal transduction. Innate Immun. *26*, 4–14. https://doi.org/10.1177/1753425919852695.
50. Chattopadhyay, R., Mani, A.M., Singh, N.K., and Rao, G.N. (2018). Resolvin D1 blocks H(2)O(2)-mediated inhibitory crosstalk between SHP2 and PP2A and suppresses endothelial-monocyte interactions. Free Radic. Biol. Med. *117*, 119–131. https://doi.org/10.1016/j.freeradbiomed.2018.01.034.
51. Dollery, C.M., Owen, C.A., Sukhova, G.K., Krettek, A., Shapiro, S.D., and Libby, P. (2003). Neutrophil elastase in human atherosclerotic plaques: production by macrophages. Circulation *107*, 2829–2836. https://doi.org/10.1161/01.CIR.0000072792.65250.4A.
52. Wen, G., An, W., Chen, J., Maguire, E.M., Chen, Q., Yang, F., Pearce, S.W.A., Kyriakides, M., Zhang, L., Ye, S., et al. (2018).

Genetic and Pharmacologic Inhibition of the Neutrophil Elastase Inhibits Experimental Atherosclerosis. J. Am. Heart Assoc. *7*, e008187. https://doi.org/10.1161/JAHA.117.008187.

53. Papayannopoulos, V., Metzler, K.D., Hakkim, A., and Zychlinsky, A. (2010). Neutrophil elastase and myeloperoxidase regulate the formation of neutrophil extracellular traps. J. Cell Biol. *191*, 677–691. https://doi.org/10.1083/jcb.201006052.
54. Geng, S., Zhang, Y., Lee, C., and Li, L. (2019). Novel reprogramming of neutrophils modulates inflammation resolution during atherosclerosis. Sci. Adv. *5*, eaav2309. https://doi.org/10.1126/sciadv.aav2309.
55. Nishio, S., Teshima, Y., Takahashi, N., Thuc, L.C., Saito, S., Fukui, A., Kume, O., Fukunaga, N., Hara, M., Nakagawa, M., and Saikawa, T. (2012). Activation of CaMKII as a key regulator of reactive oxygen species production in diabetic rat heart. J. Mol. Cell. Cardiol. *52*, 1103–1111. https://doi.org/10.1016/j.yjmcc.2012.02.006.
56. Lu, S., Liao, Z., Lu, X., Katschinski, D.M., Mercola, M., Chen, J., Heller Brown, J., Molkentin, J.D., Bossuyt, J., and Bers, D.M. (2020). Hyperglycemia Acutely Increases Cytosolic Reactive Oxygen Species via O-linked GlcNAcylation and CaMKII Activation in Mouse Ventricular Myocytes. Circ. Res. *126*, e80–e96. https://doi.org/10.1161/CIRCRESAHA.119.316288.
57. Dixit, E., Boulant, S., Zhang, Y., Lee, A.S.Y., Odendall, C., Shum, B., Hacohen, N., Chen, Z.J., Whelan, S.P., Fransen, M., et al. (2010). Peroxisomes are signaling platforms for antiviral innate immunity. Cell *141*, 668–681. https://doi.org/10.1016/j.cell.2010.04.018.
58. Di Cara, F., Andreoletti, P., Trompier, D., Vejux, A., Bülow, M.H., Sellin, J., Lizard, G., Cherkaoui-Malki, M., and Savary, S. (2019). Peroxisomes in Immune Response and Inflammation. Int. J. Mol. Sci. *20*, 3877. https://doi.org/10.3390/ijms20163877.
59. Bakele, M., Joos, M., Burdi, S., Allgaier, N., Pöschel, S., Fehrenbacher, B., Schaller, M., Marcos, V., Kümmerle-Deschner, J., Rieber, N., et al. (2014). Localization and functionality of the inflammasome in neutrophils. J. Biol. Chem. *289*, 5320–5329. https://doi.org/10.1074/jbc.M113.505636.
60. Shipley, J.M., and Waxman, D.J. (2003). Down-regulation of STAT5b transcriptional activity by ligand-activated peroxisome proliferator-activated receptor (PPAR) alpha and PPARgamma. Mol. Pharmacol. *64*, 355–364. https://doi.org/10.1124/mol.64.2.355.
61. Hogan, J.C., and Stephens, J.M. (2001). The identification and characterization of a STAT 1 binding site in the PPARgamma2 promoter. Biochem. Biophys. Res. Commun. *287*, 484–492. https://doi.org/10.1006/bbrc.2001.5606.
62. Ricote, M., Li, A.C., Willson, T.M., Kelly, C.J., and Glass, C.K. (1998). The peroxisome proliferator-activated receptor-gamma is a negative regulator of macrophage activation. Nature *391*, 79–82. https://doi.org/10.1038/34178.
63. Rhee, S.G., and Bae, S.H. (2015). The antioxidant function of sestrins is mediated by promotion of autophagic degradation of Keap1 and Nrf2 activation and by inhibition of mTORC1. Free Radic. Biol. Med. *88*, 205–211. https://doi.org/10.1016/j.freeradbiomed.2015.06.007.
64. Lin, R., Zhang, Y., Pradhan, K., and Li, L. (2020). TICAM2-related pathway mediates neutrophil exhaustion. Sci. Rep. *10*, 14397. https://doi.org/10.1038/s41598-020-71379-y.
65. Burn, G.L., Foti, A., Marsman, G., Patel, D.F., and Zychlinsky, A. (2021). The Neutrophil. Immunity *54*, 1377–1391. https://doi.org/10.1016/j.immuni.2021.06.006.
66. Rosales, C. (2018). Neutrophil: A Cell with Many Roles in Inflammation or Several Cell Types? Front. Physiol. *9*, 113. https://doi.org/10.3389/fphys.2018.00113.
67. Chu, D., Dong, X., Shi, X., Zhang, C., and Wang, Z. (2018). Neutrophil-Based Drug Delivery Systems. Adv. Mater. *30*, e1706245. https://doi.org/10.1002/adma.201706245.
68. Song, Z., Bhattacharya, S., Clemens, R.A., and Dinauer, M.C. (2023). Molecular regulation of neutrophil swarming in health and disease: Lessons from the phagocyte oxidase. iScience *26*, 108034. https://doi.org/10.1016/j.isci.2023.108034.
69. Nauseef, W.M., and Borregaard, N. (2014). Neutrophils at work. Nat. Immunol. *15*, 602–611. https://doi.org/10.1038/ni.2921.
70. Herrero-Cervera, A., Soehnlein, O., and Kenne, E. (2022). Neutrophils in chronic inflammatory diseases. Cell. Mol. Immunol. *19*, 177–191. https://doi.org/10.1038/s41423-021-00832-3.
71. Rawat, K., and Shrivastava, A. (2022). Neutrophils as emerging protagonists and targets in chronic inflammatory diseases. Inflamm. Res. *71*, 1477–1488. https://doi.org/10.1007/s00011-022-01627-6.
72. Peiseler, M., and Kubes, P. (2019). More friend than foe: the emerging role of neutrophils in tissue repair. J. Clin. Invest. *129*, 2629–2639. https://doi.org/10.1172/JCI124616.
73. Grayson, P.C., Schauer, C., Herrmann, M., and Kaplan, M.J. (2016). Review: Neutrophils as Invigorated Targets in Rheumatic Diseases. Arthritis Rheumatol. *68*, 2071–2082. https://doi.org/10.1002/art.39745.
74. Gullotta, G.S., De Feo, D., Friebel, E., Semerano, A., Scotti, G.M., Bergamaschi, A., Butti, E., Brambilla, E., Genchi, A., Capotondo, A., et al. (2023). Age-induced alterations of granulopoiesis generate atypical neutrophils that aggravate stroke pathology. Nat. Immunol. *24*, 925–940. https://doi.org/10.1038/s41590-023-01505-1.
75. Dahlstrand Rudin, A., Amirbeagi, F., Davidsson, L., Khamzeh, A., Thorbert Mros, S., Thulin, P., Welin, A., Björkman, L., Christenson, K., and Bylund, J. (2021). The neutrophil subset defined by CD177 expression is preferentially recruited to gingival crevicular fluid in periodontitis. J. Leukoc. Biol. *109*, 349–362. https://doi.org/10.1002/JLB.3A0520-081RR.
76. Levy, Y., Wiedemann, A., Hejblum, B.P., Durand, M., Lefebvre, C., Surenaud, M., Lacabaratz, C., Perreau, M., Foucat, E., Dechenaud, M., et al. (2021). CD177, a specific marker of neutrophil activation, is associated with coronavirus disease 2019 severity and death. iScience *24*, 102711. https://doi.org/10.1016/j.isci.2021.102711.
77. Fredman, G., Ozcan, L., Spolitu, S., Hellmann, J., Spite, M., Backs, J., and Tabas, I. (2014). Resolvin D1 limits 5-lipoxygenase nuclear localization and leukotriene B4 synthesis by inhibiting a calcium-activated kinase pathway. Proc. Natl. Acad. Sci. USA *111*, 14530–14535. https://doi.org/10.1073/pnas.1410851111.
78. Luo, M., Jones, S.M., Peters-Golden, M., and Brock, T.G. (2003). Nuclear localization of 5-lipoxygenase as a determinant of leukotriene B4 synthetic capacity. Proc. Natl. Acad. Sci. USA *100*, 12165–12170. https://doi.org/10.1073/pnas.2133253100.
79. Henriksen, P.A., and Sallenave, J.M. (2008). Human neutrophil elastase: mediator and therapeutic target in atherosclerosis. Int. J. Biochem. Cell Biol. *40*, 1095–1100. https://doi.org/10.1016/j.biocel.2008.01.004.
80. Yamamoto, M., Sato, S., Hemmi, H., Uematsu, S., Hoshino, K., Kaisho, T., Takeuchi, O., Takeda, K., and Akira, S. (2003). TRAM is specifically involved in the Toll-like receptor 4-mediated MyD88-independent signaling pathway. Nat. Immunol. *4*, 1144–1150. https://doi.org/10.1038/ni986.
81. Ruysschaert, J.M., and Lonez, C. (2015). Role of lipid microdomains in TLR-mediated signalling. Biochim. Biophys. Acta *1848*, 1860–1867. https://doi.org/10.1016/j.bbamem.2015.03.014.
82. Rowe, D.C., McGettrick, A.F., Latz, E., Monks, B.G., Gay, N.J., Yamamoto, M., Akira, S., O'Neill, L.A., Fitzgerald, K.A., and Golenbock, D.T. (2006). The myristoylation of TRIF-related adaptor molecule is essential for Toll-like receptor 4 signal transduction. Proc. Natl. Acad. Sci. USA *103*, 6299–6304. https://doi.org/10.1073/pnas.0510041103.
83. Shentu, T.P., Titushkin, I., Singh, D.K., Gooch, K.J., Subbaiah, P.V., Cho, M., and Levitan, I. (2010). oxLDL-induced decrease in lipid order of membrane domains is inversely correlated with endothelial stiffness and network formation. Am. J. Physiol. Cell Physiol. *299*, C218–C229. https://doi.org/10.1152/ajpcell.00383.2009.
84. Smith, P., Jeffers, L.A., and Koval, M. (2021). Measurement of Lung Vessel and Epithelial Permeability In Vivo with Evans Blue. Methods Mol. Biol. *2367*, 137–148. https://doi.org/10.1007/7651_2020_345.
85. Bolte, S., and Cordelières, F.P. (2006). A guided tour into subcellular colocalization analysis in light microscopy. J. Microsc. *224*, 213–232. https://doi.org/10.1111/j.1365-2818.2006.01706.x.
86. Hopke, A., Scherer, A., Kreuzburg, S., Abers, M.S., Zerbe, C.S., Dinauer, M.C., Mansour, M.K., and Irimia, D. (2020). Neutrophil swarming delays the growth of clusters of pathogenic fungi. Nat. Commun. *11*, 2031. https://doi.org/10.1038/s41467-020-15834-4.

STAR★METHODS

KEY RESOURCES TABLE

REAGENT or RESOURCE	SOURCE	IDENTIFIER
Antibodies		
Purified rat anti-mouse CD16/CD32 (Fc block)	BD Biosciences	Cat# 553141; RRID: AB_394656
APC/Cyanine7 anti-mouse/human CD11b (Clone M1/70)	BioLegend	Cat# 101226; RRID: AB_830642
PE/Cyanine7 anti-mouse Ly6C (Clone HK1.4)	BioLegend	Cat# 128018; RRID: AB_1732093
PE anti-mouse Ly6G (Clone 1A8)	BioLegend	Cat# 127608; RRID: AB_1186104
Alexa Fluor 647 anti-mouse Ly-6G (Clone 1A8)	BioLegend	Cat# 127610; RRID: AB_1134159
FITC anti-mouse Ly-6G (Clone 1A8)	BioLegend	Cat# 127606; RRID: AB_1236488
FITC anti-mouse CD45 (Clone 30-F11)	BioLegend	Cat# 103108; RRID: AB_312972
Alexa Fluor 647 anti-mouse VCAM-1 (Clone 429)	BioLegend	Cat# 105712; RRID: AB_493429
PE anti-mouse CD31 (Clone W18222B)	BioLegend	Cat# 160204; RRID: AB_2860750
APC anti-mouse ICAM1 (Clone YN1/1.7.4)	BioLegend	Cat# 116120; RRID: AB_10613645
PE anti-mouse CD38 (Clone 90)	BioLegend	Cat# 102708; RRID: AB_312929
Alexa Fluor 647 anti-rat IgG2a (Clone MRG2a-83)	BioLegend	Cat# 407512; RRID: AB_2716140
APC anti-human VCAM-1 (Clone STA)	BioLegend	Cat# 305810; RRID: AB_2214226
HRP anti-mouse β-actin (Clone 13E5)	Cell Signaling Technology	Cat# 5125; RRID: AB_1903890
Anti-mouse FLAP (polyclonal)	Thermo Fisher Scientific	Cat# PA5-78368; RRID: AB_2735780
Anti-mouse SESN1 (Clone ARC2313)	Thermo Fisher Scientific	Cat# MA5-38000; RRID: AB_2897918
HRP anti-rabbit IgG	Cell Signaling Technology	Cat# 7074; RRID: AB_2099233
Cy3 anti-mouse LAMP1 (polyclonal)	Abcam	Cat# ab67283; RRID: AB_1140882
Alexa Fluor 546 anti-mouse CaMKII (clone G-1)	Santa Cruz	Cat# sc-5306 AF546; RRID: AB_626788
PE anti-mouse SYK (Clone 5F5)	BioLegend	Cat# 646004; RRID: AB_2565306
Biotin anti-mouse LOX5 (polyclonal)	NOVUS	Cat# NB110-58748B; RRID: AB_920580
Biotin anti-mouse TRAM (polyclonal)	Biorbyt	Cat# orb452158; RRID: NA
FITC anti-human CD66b (Clone G10F5)	BioLegend	Cat# 305104; RRID: AB_314495
PE anti-human CD177 (Clone MEM-166)	BioLegend	Cat# 315806; RRID: AB_2564280
Goat anti-FLAP (polyclonal)	NOVUS	Cat# NB300-891; RRID: AB_2227081
Mouse anti-CaMKII (Clone G-1)	Santa Cruz	Cat# sc-5306; RRID: AB_626788
Rabbit anti-SYK (polyclonal)	Cell Signaling Technology	Cat# 2712; RRID: AB_2197223
Alexa Fluor 647 anti-goat IgG secondary antibody	Thermo Fisher Scientific	Cat# A56570; RRID: AB_2930909
Alexa Fluor 647 anti-human TRAM (Clone E−2)	Santa Cruz	Cat# sc-376076; RRID: AB_10989356
Chemicals, peptides, and recombinant proteins		
Hematoxylin solution	Sigma-Aldrich	Cat# GHS132
Eosin Y solution	Sigma-Aldrich	Cat# HT110132
High fat diet	Harlan Teklad	Cat# 94059
Formalin	Fisher Scientific	Cat# SF100-4
OCT Compound	Sakura Finetek	Cat# 4583
Collagenase, Type I	Worthington	Cat# LS004196
Collagenase, Type XI	Sigma-Aldrich	Cat# C7657

(*Continued on next page*)

Continued

REAGENT or RESOURCE	SOURCE	IDENTIFIER
ACK buffer	Thermo Fisher Scientific	Cat# A1049201
ACK buffer	Quality Biological	Cat# 118156721
Hyaluronidase	Sigma-Aldrich	Cat# H6254
Deoxyribonuclease	Sigma-Aldrich	Cat# DN25
HEPES solution	Sigma-Aldrich	Cat# H0887
Propidium iodide	Sigma-Aldrich	Cat# P4170
RPMI-1640 medium	Sigma-Aldrich	Cat# R8758
DMEM	Sigma-Aldrich	Cat# D6429
Recombinant murine G-CSF	Peprotech	Cat# AF-250-05
PBS	Thermo Fisher Scientific	Cat# 10010023
FBS	GE Healthcare HyClone	Cat# SH3007003
HBSS	Sigma	Cat# H6648
L-Glutamine	Thermo Fisher Scientific	Cat# 25030081
Penicillin-streptomycin	Thermo Fisher Scientific	Cat# 15-140-122
oxLDL	Kalen Biomedical	Cat# 770202-6
Cholesterol-water soluble	Sigma-Aldrich	Cat# C49516
Canada balsam	Sigma-Aldrich	Cat# C1795
Permount™ mounting medium	Thermo Fisher Scientific	Cat# SP15-500
CellROX green reagent	Thermo Fisher Scientific	Cat# C10444
RIPA buffer	Thermo Fisher Scientific	Cat# 89900
Blotting-grade blocker	Bio-Rad	Cat# 1706404
Protease inhibitor cocktail	Sigma-Aldrich	Cat# P8340
Antifade mountant	Thermo Fisher Scientific	Cat# P36930
Evans Blue	Sigma-Aldrich	Cat# E2129
Human TruStain FcX™ (Fc Receptor Blocking Solution)	BioLegend	Cat# 422302
Streptavidin/Biotin Blocking Solution	Thermo Fisher Scientific	Cat# R37628
Cy3 Streptavidin	BioLegend	Cat# 405215
Alexa Fluor 488 Streptavidin	Thermo Fisher Scientific	Cat# S32354
Cyto-Fast™ Fix/Perm Buffer	BioLegend	Cat# 426803
fMLP	Sigma	Cat# 47729
Dextran	MP biomedicals	Cat# 101514
DRAQ5	BioLegend	Cat# 424101
Hoechst 33342	Thermo Fisher Scientific	Cat# 62249
DAPI	Thermo Fisher Scientific	Cat# 62248
BOC2	Phoenix Pharmaceuticals	Cat# 072-01
CFSE	Thermo Fisher Scientific	Cat# C34554
Critical commercial assays		
Fat, Oil Red O, propylene glycol stain kit	Newcomer Supply	Cat# 9119A
Picrosirius Red stain kit	Polysciences	Cat# 24901
RvD1 ELISA kit	Cayman Chemical	Cat# 500380
LTB4 Parameter Assay kit	R&D Systems	Cat# KGE006B
Mouse Elastase/ELA2 Quantikine ELISA kit	R&D Systems	Cat# MELA20
Human Elastase/ELA2 DuoSet ELISA kit	R&D Systems	Cat# DY9167
MPO ELISA kit	Thermo Fisher Scientific	Cat# EMMPO

(*Continued on next page*)

Continued

REAGENT or RESOURCE	SOURCE	IDENTIFIER
SelectFX Alexa Fluor 488 peroxisome labeling kit	Thermo Fisher Scientific	Cat# S34201
ECL Western blotting substrate	Thermo Fisher Scientific	Cat# 32209
TNFα ELISA kit	R&D Systems	Cat# MTA00B
CCL5 ELISA kit	R&D Systems	Cat# MMR00
Cholesterol quantitation kit	Sigma	Cat# MAK043
Triglyceride assay kit	BioVison	Cat# K622
Deposited data		
Single-cell RNA-seq data	This paper	GEO: GSE182356
Raw numerical data	This paper	Mendeley Data, https://doi.org/10.17632/kwbwsmkbs2.1
Experimental models: Cell lines		
HUVEC	ATCC	CRL-1730
bEnd.3	ATCC	CRL-2299
Immortalized mouse cardiac endothelial cells (MCECs)	Gift from Dr. Tianqing Peng (University of Western Ontario)	NA
Experimental models: Organisms/strains		
Mouse, C57BL/6	The Jackson Laboratory	JAX 000664
Mouse, ApoE$^{-/-}$	The Jackson Laboratory	JAX 002052
Mouse, Tram$^{-/-}$	Gift from Dr. Holger Eltzschig (University of Texas Health Science Center at Houston)	NA
Mouse, ApoE$^{-/-}$ Tram$^{-/-}$	ApoE$^{-/-}$ x Tram$^{-/-}$ in this lab	NA
Software and algorithms		
FlowJo	Tree Star	https://www.flowjo.com/
ImageJ	NIH	https://imagej.nih.gov/ij/
Prism	GraphPad	https://www.graphpad.com/scientificsoftware/prism/
ZEN lite	ZEISS	https://www.zeiss.com/microscopy/us/products/microscope-software/zen-lite.html
10x Cell Ranger v3.0.2	10X Genomics	https://support.10xgenomics.com/single-cell-gene-expression/software/overview/welcome
Other		
Transwell inserts (0.4 μm)	Corning	Cat# 353180
Cell strainer (70 μm)	Fisher Scientific	Cat# 22-363-548

RESOURCE AVAILABILITY

Lead contact

Further information and requests for resources and reagents should be directed to and will be fulfilled by the lead contact, Liwu Li (lwli@vt.edu).

Materials availability

This study did not generate any unique reagents.

Data and code availability

- The underlying numerical data and western blot original figures were deposited on Mendeley Data, https://doi.org/10.17632/kwbwsmkbs2.1.

- Processed single-cell RNA-seq data have been previously published.[28] The raw data were deposited at GEO with the accession number GSE182356.
- This paper did not report the original code.
- All data analyzed during this study have been included in the manuscript and supporting files. Any additional information required to reanalyze the data reported in this paper is available from the lead contact upon request.

EXPERIMENTAL MODEL AND STUDY PARTICIPANT DETAILS

Animals and ethics statement

WT C57BL/6 and ApoE$^{-/-}$ mice were purchased from the Jackson Laboratory. Tram$^{-/-}$ mouse colony was kindly provided by Dr. Holger Eltzschig. ApoE$^{-/-}$ Tram$^{-/-}$ mice were obtained by crossing ApoE$^{-/-}$ mice with Tram$^{-/-}$ mice. All mice were maintained on a 12h/12h light/dark cycle at 22°C in a pathogen-free environment. All experimental procedures were approved by the Intuitional Animal Care and Use Committee of Virginia Tech in compliance with the US National Institutes of Health Guide for the Care and Use of Laboratory Animals. Both male and female mice between 8 and 12 weeks of age group were used for experiments, and no gender-specific effects were observed.

METHOD DETAILS

Primary murine neutrophil culture

BM cells were harvested from the femur and tibia of mice, and Ly6G^{+} neutrophils in the BM were sorted by flow cytometry. The neutrophils were cultured in complete RPMI 1640 medium (containing 10% FBS, 2 mM L-glutamine, penicillin-streptomycin) supplemented with G-CSF (100 ng/mL). In some experiments, neutrophils were treated with oxLDL (10 μg/mL), or free cholesterol (10 μg/mL) for 48 h.

Human neutrophils isolation

Peripheral blood from healthy donors was commercially purchased from Research Blood Components LLC. Human neutrophils were isolated by dextran sedimentation and FACS (fluorescence-activated cell sorting). Briefly, whole blood was mixed with 3% Dextran at 1:1 ratio for 30 min at room temperature. The upper layer containing leukocytes was harvested, and residual red blood cells were removed by ACK lysis buffer. Then, leukocytes were blocked with Fc blocker in FACS buffer (2% FBS in 1xHBSS) for 15 min, and then labeled with fluorescent-conjugated anti-CD66b and anti-CD177 antibodies for 30 min. Propidium iodide (PI) was added to separate live and dead cells. PI^{-}CD66b^{+}CD177^{lo} and PI^{-}CD66b^{+}CD177^{hi} were sorted by Sony cell sorter SH800. Purified neutrophils were resuspended in RPMI1640 complete medium for further use.

Cell lines

Three different endothelial cell lines were used in this study. HUVECs and bEnd.3 cells were purchased from ATCC; immortalized mouse cardiac endothelial cells (MCECs) were provided by Dr. Tianqing Peng at the University of Western Ontario. All the endothelial cell lines were cultured in DMEM with 10% FBS and penicillin-streptomycin.

HFD feeding and neutrophil adoptive transfer

Age and gender-matched recipient ApoE$^{-/-}$ Tram$^{+/+}$ mice were fed with HFD for 4 weeks to induce the development of atherosclerosis. Ly6G^{+} neutrophils were sorted from the BM of ApoE$^{-/-}$ Tram$^{-/-}$ mice or control ApoE$^{-/-}$ Tram$^{+/+}$ mice using flow cytometry. Adoptive transfer of neutrophils was conducted as described previously.[54] Each HFD-fed recipient mouse was transfused with 2 × 10^{6} neutrophils in 200 μL of PBS once weekly through intravenous injection for a total of 4 injections. The mice were continuously maintained on HFD throughout the adoptive transfer regimen. One week after the final cell transfer, the mice were sacrificed, and tissues were harvested for subsequent analyses.

Histological analyses of atherosclerotic lesions

Histological analyses of atherosclerotic lesions were performed as previously described.[54] Briefly, fresh-frozen and optimal cutting temperature (OCT) compound–embedded proximal aortic sections (10 μm) were fixed in 4% neutral buffered formalin followed by H&E staining. Oil Red O staining was performed using a kit (Newcomer Supply), and collagen staining was performed using the Picrosirius Red Stain Kit (Polysciences) according to the manufacturer's instructions. The samples were mounted with Canada balsam or Permount mounting medium and observed under a light microscope. Quantification of the samples was performed with ImageJ. The percentages of total lesion area, lipid deposition, and collagen composition were calculated.

ELISA

Plasma samples were collected from the mice that received neutrophil transfer. The levels of RvD1, elastase, LTB4, MPO, TNFα, and CCL5 were determined with commercially available ELISA kits. For the analysis of RvD1 and elastase levels in cell culture supernatant, Ly6G^{+} neutrophils were sorted from the BM of Tram$^{-/-}$ mice and WT mice and then treated with oxLDL (10 μg/mL) for 48 h. The resulting supernatant was collected for the quantification of RvD1 and elastase. Sorted human neutrophils were plated into 96-well plates and stimulated with or

without fMLP (100 nM) for 4 h, then the supernatant was collected to determine LTB4 and elastase levels. All the assays were conducted following the manufacturers' instructions. Detailed information of the ELISA kits can be found in the key resources table.

Determination of plasma lipids

Plasma samples were collected from the mice that received neutrophil transfer. Total and free cholesterol levels as well as triglyceride level were quantified using with commercially available kits. All assays were performed according to the manufacturers' instructions, and detailed information of the kits can be found in the key resources table.

Flow cytometry analysis of aortic neutrophils

Age and gender-matched recipient ApoE$^{-/-}$ Tram$^{+/+}$ mice were fed with HFD for 4 weeks, and neutrophils were sorted from ApoE$^{-/-}$ Tram$^{-/-}$ mice or ApoE$^{-/-}$ Tram$^{+/+}$ mice as decribed above. The purified neutrophils were labeled with CFSE before adoptive transfer. Each HFD-fed recipient mouse was transfused with 2 × 10^{6} CFSE-labeled neutrophils once weekly through intravenous injection for a total of 4 injections. The mice were continuously maintained on HFD throughout the adoptive transfer regimen. One day after the final cell transfer, the mice were sacrificed, and total neutrophils and CFSE^{+} neutrophils in the aorta were analyzed with flow cytometry.

Assessment of aortic endothelium permeability

The aortic endothelium permeability was determined using an established protocol with modifications.[84] ApoE$^{-/-}$ Tram$^{+/+}$ mice were transfused with ApoE$^{-/-}$ Tram$^{-/-}$ or control ApoE$^{-/-}$ Tram$^{+/+}$ neutrophils as described above. One week post the final cell transfer, 200 μL of 0.5% Evans Blue solution (in PBS) was intravenously injected into each recipient mouse. After 1 h, the mouse was sacrificed, and the blood and aorta were collected. The serum was prepared and preserved at −20°C. The aorta was rinsed with PBS, weighted, and put in a conical microfuge tube containing 250 μL of formamide, followed by incubation at 55°C for 48 h. The aorta sample was centrifugated, and the supernatant was collected. The absorbance of serum and aorta supernatant samples and Evans Blue standards was measured at 620 nm. The Evans Blue concentrations in the serum and aorta samples were calculated. The Evans Blue concentration of aorta sample was divided by aorta weight and then by serum Evans Blue concentration for normalization.

Flow cytometry analysis of aortic endothelial cells

ApoE$^{-/-}$ Tram$^{+/+}$ mice were transfused with ApoE$^{-/-}$ Tram$^{-/-}$ or ApoE$^{-/-}$ Tram$^{+/+}$ neutrophils as described above. One week after the final neutrophil transfer, aortas were harvested, and single-cell suspensions were prepared for flow cytometry as previously reported.[23] Aortas were cut into small pieces and then transferred into an enzyme cocktail (in HBSS) containing 450 U/ml collagenase type I, 250 U/ml collagenase type XI, 120 U/ml hyaluronidase and 120 U/ml DNAse supplemented with 20 mM HEPES. The samples were incubated at 37°C for 60 min. The processed samples of all tissues were filtered through 70-μm cell strainers to obtain single-cell suspension, and red blood cells were lysed with ACK buffer. The samples were incubated with anti-CD16/-CD32 antibody to block Fc-receptors, followed by staining with fluorochrome-conjugated anti-CD45, anti-CD31, and anti-VCAM-1 antibodies. PI was added before flow cytometry to label dead cells. The expression of VCAM-1 on the surface of PI^{-} CD45^{-} CD31^{+} endothelial cells was examined using FACSCanto II (BD Biosciences). The data were analyzed using FlowJo. Detailed information on the antibodies and reagents can be found in the key resources table.

Flow cytometry analysis of bone marrow and splenic monocytes

ApoE$^{-/-}$ Tram$^{+/+}$ mice were transfused with ApoE$^{-/-}$ Tram$^{-/-}$ or ApoE$^{-/-}$ Tram$^{+/+}$ neutrophils as described above. One week after the final neutrophil transfer, bone marrow and spleen were harvested, and single-cell suspensions were prepared for flow cytometry as previously reported.[23] After lysing red blood cells, the samples were incubated with anti-CD16/-CD32 antibody to block Fc-receptors, followed by staining with fluorochrome-conjugated anti-CD11b, anti-Ly6G, anti-Ly6C, anti-ICAM1 and anti-CD38 antibodies. PI was added before flow cytometry to label dead cells. The expressions of ICAM1 and CD38 on the surface of PI^{-} CD11b^{+} Ly6G^{-} Ly6C^{++}, PI^{-} CD11b^{+} Ly6G^{-} Ly6C^{+}, and PI^{-} CD11b^{+} Ly6G^{-} Ly6C^{-} monocyte subsets were examined using FACSCanto II (BD Biosciences). The data were analyzed using FlowJo. Detailed information on the antibodies and reagents can be found in the key resources table.

Assessment of the viability of neutrophils cultured *in vitro*

Ly6G^{+} neutrophils were sorted from the BM of Tram$^{-/-}$ mice and WT mice and then treated with oxLDL (10 μg/mL) for 24 or 48 h. The neutrophils were harvested and labeled with PI. The viability of neutrophils was assessed using FACSCanto II (BD Biosciences).

Neutrophil-endothelial cell co-culture, Transwell-Evans Blue permeability assay, and flow cytometry analysis

Ly6G^{+} neutrophils were sorted from the BM of Tram$^{-/-}$ mice and WT mice. To determine the effect of neutrophils on the integrity of the endothelial cell layer, a Transwell-Evans Blue permeability assay was conducted according to previously established protocol with modifications.[42,43] Briefly, bEnd.3 cells or MCECs were seeded to each Transwell insert (0.4 μm pore size) for 12-well plates and cultured for 24 h to form a monolayer. Tram$^{-/-}$ or WT neutrophils were added to the insert at a 10:1 ratio (neutrophils to endothelial cells), followed by co-culture for 24 h. In some experiments the monolayer of MCECs was pre-incubated with BOC2 (10 μM) or vehicle buffer (0.8% MeOH) for 1 h before adding neutrophils. The medium in the insert was discarded, the insert was transferred to a new 12-well plate containing 4% BSA, and 400 μL of Evans

Blue solution (0.67 ng/mL) was added to the insert. After incubation for 30 min, the absorbance of the medium in the lower chamber of the Transwell system was measured at 620 nm, allowing for the quantification of Evans Blue leakage. Evans Blue leakage to the lower chamber of Transwell system that only contained endothelial cell monolayer without adding neutrophils was employed for normalization. To examine the expression of VCAM-1 on endothelial cells, HUVECs, bEnd.3 cells or MCECs were seeded to 12-well plates and cultured for 24 h to form a monolayer. Tram$^{-/-}$ or WT neutrophils were co-cultured with endothelial cells at a 10:1 ratio. In some experiments the monolayer of MCECs was pre-incubated with BOC2 (10 μM) or vehicle buffer (0.8% MeOH) for 1 h before adding neutrophils. After 24 h, cells were harvested, blocked with anti-CD16/-CD32 antibody, and stained with fluorochrome-conjugated anti-Ly6G and anti-VCAM-1 antibodies. PI was added before flow cytometry. The expression of VCAM-1 on the surface of PI$^-$ Ly6G$^-$ endothelial cells was examined using FACSCanto II (BD Biosciences). The death of endothelial cells was also assessed by flow cytometry based on PI staining.

Assessment of the infleuce of neutrophils on endothrelial cells without direct cell-cell contact

MCECs were seeded to the lower chamber of 12-well plates containing a Transwell insert (0.4 μm pore size) in each well and cultured for 24 h to form a monolayer. Ly6G$^+$ neutrophils were sorted from the BM of Tram$^{-/-}$ mice and WT mice and then seeded to the upper chamber of the Transwell insert (ratio of neutrophils to MCECs = 10:1). In parallel, WT and Tram$^{-/-}$ neutrophils were co-cultured with MCECs at 10:1 ratio without Transwell insert separation as decribed above. After 24 h, cells were harvested, blocked with anti-CD16/-CD32 antibody, and stained with fluorochrome-conjugated anti-Ly6G and anti-VCAM-1 antibodies. PI was added before flow cytometry. The expression of VCAM-1 on the surface of PI$^-$ Ly6G$^-$ MCECs was examined using FACSCanto II (BD Biosciences). The death of MCECs was also assessed by flow cytometry based on PI staining.

Immunoblotting

Ly6G$^+$ neutrophils were sorted from the BM of Tram$^{-/-}$ mice and WT mice and then treated with oxLDL (10 μg/mL) for 48 h. Total proteins were extracted with RIPA buffer containing a protease inhibitor cocktail. The same amount of protein samples were subjected to SDS-PAGE and transferred to a polyvinylidene difluoride membrane, which was then incubated with blocker at room temperature for 1 h. The membrane was incubated with primary anti-FLAP, anti-SESN1, anti-CamKII, anti-SYK or anti-β-actin antibody overnight at 4°C, followed by incubation with horseradish peroxidase (HRP)-conjugated anti-rabbit IgG for 1 h at room temperature. Blots were developed using a chemiluminescence ECL detection kit. Detailed information on the antibodies and reagents can be found in the key resources table.

Confocal microscopy

Ly6G$^+$ neutrophils were sorted from the BM of Tram$^{-/-}$ mice and WT mice and then treated with oxLDL (10 μg/mL) or free cholesterol (10 μg/mL) for 48 h. Peroxisome-lysosome fusion in neutrophils was examined by confocal microscopy with a protocol as previously reported.[54] Neutrophils were fixed with 4% paraformaldehyde, deposited on slides by cytospin, and permeabilized with 0.2% Triton X-100. The samples were then blocked and stained with primary rabbit anti-mouse PMP70 antibody followed by staining with Alexa Fluor 488-conjugated goat anti-rabbit secondary antibody to label peroxisomes. The blocking solution and antibodies were supplied in the SelectFX Alexa Fluor 488 Peroxisome Labeling Kit. After extensive washing with PBS, the cells were stained with Cy3-conjugated anti-LAMP1 antibody to label lysosomes. To detect the lysosomal distribution of CaMKII and SYK, peroxisomes in the neutrophils were first labeled as described above. After washing with PBS, the neutrophils were stained with Alexa Fluor 546-conjugated anti-CaMKII antibody or PE conjugated anti-SYK antibody. To observe the intracellular distribution of LOX5 and TRAM, neutrophils were fixed, deposited on slides, permeabilized, and blocked with Streptavidin/Biotin Blocking Solution. The samples were then stained with biotin-conjugated anti-LOX5 antibody or biotin-conjugated anti-TRAM antibody, followed by Cy3-conjugated streptavidin or Alexa Fluor 488-conjugated streptavidin, respectively. The nuclei were counterstained with DAPI. All the samples were mounted with antifade mountant and observed under LSM 900 confocal microscope (ZEISS). Images were processed with ZEN lite. The co-localization of intracellular molecules was analyzed using ImageJ plugin JACoP and quantified according to Pearson's coefficient for each cell.[85] Detailed information on the antibodies and reagents can be found in the key resources table.

Detection of intracellular ROS

Ly6G$^+$ neutrophils were sorted from the BM of Tram$^{-/-}$ mice and WT mice and then treated with oxLDL (10 μg/mL) for 48 h. Intracellular ROS level was determined with the method described previously.[54] CellROX Green Reagent was added to neutrophil cultures 30 min before harvesting. The samples were examined using FACSCanto II, and the data were analyzed using FlowJo.

Flow cytometry analyses of human neutrophils

Peripheral blood from healthy individuals was purchased from Research Blood Components LLC. After lysing red blood cells, the samples were blocked with Fc Receptor Blocking Solution and stained with FITC-conjugated anti-CD66b and PE-conjugated anti-CD177 antibodies. The cells were then fixed and permeabilized using Cyto-Fast Fix/Perm Buffer, followed by Alexa Fluor 647-conjugated anti-TRAM antibody staining. The expression of CD177 and TRAM in CD66b$^+$ neutrophils was examined using FACSCanto II, and the data were analyzed using FlowJo. Detailed information on the antibodies and reagents can be found in the key resources table.

Swarming assay

We prepared 1 × 3 inches slides by printing poly-L-lysine dots of 100 μm diameter spaced at 500 μm distance. We incubated zymosan particles on the slides for 10 min and washed the slides clean with PBS using a spray bottle. Following the washing step, we verified that clusters of zymosan formed on top of the printed array. We assembled the slides with multi-well attachments.[86] We prepared $CD177^{lo}$ and $CD177^{hi}$ human neutrophils by sorting as described above and fluorescently labeling each population. Specifically, we labeled $CD177^{lo}$ neutrophils with Hoechst 33342 dye at a final concentration of 10 μM and labeled $CD177^{hi}$ neutrophils with DRAQ5 dye at a final concentration of 10 μM for 15 min at 37°C. After washing the labeling dye, we resuspended the neutrophils in RPMI complete medium at a concentration of 2.5 million cells per mL. We added 200 μL of the neutrophil suspension to each well. We recorded time-lapse images at 37°C, every 2 min for 60 min, using a KEYENCE fluorescence microscope. We quantified the accumulation of neutrophils on the zymosan-cluster targets by measuring the increase in fluorescence intensity on top of the targets at 60 min using ImageJ.

QUANTIFICATION AND STATISTICAL ANALYSIS

Statistical analyses were conducted using Prism software. All data are expressed as means ± SEM, and the sample number for each dataset is provided in figure legends. Comparisons between two groups were performed using 2-tailed Student's t test, and comparisons among multiple groups were carried out with one-way ANOVA. $p < 0.05$ was considered statistically significant.